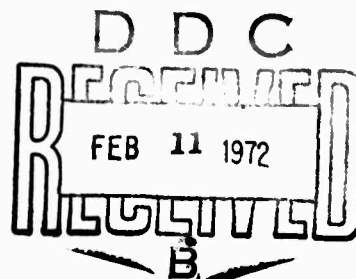AFOSR - TR - 72 - 0273

2 JAN 1972

Final Technical Report
1 November 1970 - 31 December 1971

Sponsored by
Advanced Research Projects Agency
ARPA Order No. 1705

D D C

FEB 11 1972

B

Program Code	1F10
Contractor	George Washington University
Date of Contract	1 November 1970
Date of Expiration	31 December 1971
Amount of Contract	$39,165.00
Grant Number	AFOSR-71-1985
Principal Investigator	J.W. Pierce (281-5862)
Project Scientist	S.A. Alsup (451-0052)
Short Title	Relative generation of seismic waves to 4000 Kilometers epicentral distance

Approved for public release
Distribution unlimited

DOCUMENT CONTROL DATA - R & D

(Security classification of title, body of abstract and indexing annotation must be entered when the overall report is classified)

1. ORIGINATING ACTIVITY (Corporate author)	2a. REPORT SECURITY CLASSIFICATION
The George Washington University	UNCLASSIFIED
Washington, D.C.	2b. GROUP

3. REPORT TITLE

RELATIVE GENERATION OF SEISMIC WAVES TO 4000 KILOMETERS EPICENTRAL DISTANCE:

4. DESCRIPTIVE NOTES (Type of report and inclusive dates)

Scientific........FINAL

5. AUTHOR(S) (First name, middle initial, last name)

S.A. Alsup

6. REPORT DATE	7a. TOTAL NO. OF PAGES	7b. NO. OF REFS
31 December 1971	66	64

8a. CONTRACT OR GRANT NO	9a. ORIGINATOR'S REPORT NUMBER(S)
AFOSR-71-1985	
b. PROJECT NO. AO 1705	
c. 62701D	9b. OTHER REPORT NO(S) (Any other numbers that may be assigned this report)
d.	AFOSR - TR - 72 - 0273

10. DISTRIBUTION STATEMENT

Approved for public release; distribution unlimited.

11. SUPPLEMENTARY NOTES	12. SPONSORING MILITARY ACTIVITY
TECH, OTHER	Air Force Office of Scientific Res. 1400 Wilson Boulevard (NPG) Arlington, Virginia 22209

13. ABSTRACT

Lateral variations of seismic wave absorption in the upper mantle beneath the United States are determined by calculation of seismic Q for Pn wave paths. Departures from the amplitude decay of the Pn wave predicted by cylindrical spreading along the crust-mantle boundary form the basis of the Q estimation. Sufficient paths are obtained to construct tentative contours of upper mantle Q beneath most of the United States. Agreement with previous Q determinations is found in those few places where vertical Q distributions have been determined. Agreement between the contours of upper mantle Q and other geophysical parameters is also demonstrated in some detail, particularly with teleseismic signal amplitude variations and delay time, heat flow, and the anamolous field intensities induced by geomagnetic storms.

RELATIVE GENERATION OF SEISMIC WAVES TO 4000 KILOMETERS EPICENTRAL DISTANCE

SYNOPSIS

The purpose of research conducted under this project has been to identify characteristics of seismic waves recorded at less than teleseismic distances which would indicate whether the wave source was an explosion or earthquake. The approach included measurement of seismic signals recorded within the distance range from over 30 shallow-focus continental earthquakes and several explosions which occurred at widely distributed locations within the United States. Results of the effort are summarized in maps of lateral variation in the seismic wave attenuation factor Q for the initial seismic wave observed at most continental distances. Contour patterns of the Q factor can be correlated with other geophysical factors in some detail, and the possibility of empirically relating these factors to Q over a broad continental region now exists.

The following report includes a description of a simple method for estimating upper mantle Q from amplitudes of the Pn seismic wave, contours of upper mantle Q beneath the United States derived by the method, and comparisons of the contours with other geophysical parameters of interest. Some immediate potential of the results toward improvement in seismic discrimination are given below.

Section 7 in the report shows an example of Pn amplitude prediction utilizing the Q contours which results in amplitudes very close to those observed at all but a few stations. This result shows that considerable reduction in the scatter of body wave magnitudes (m_b) computed from observations of the Pn signal is possible, and a much more stable (and accurate) estimate of seismic magnitude or equivalent yields may be obtained. A significant improvement in the "standard discriminant" of the difference between body wave and surface wave magnitudes (m_b, M_s) for

explosions and earthquake populations may result, especially in the events with body wave magnitude less than 4.0 where paths less than teleseismic become important to signal detection capabilities (see Semi-Annual Report #1, this contract).

Correlation of the upper mantle Q contours with teleseismic signal characteristics (Section 7.) suggests that if amplitude or traveltime variations of teleseismic data are available, an estimate of upper mantle Q may be possible without Pn observations. If the accuracy of Q is sufficient by this method, it may be possible to also estimate the influence of the Q upon seismic surface wave propagation in the wave period range where data for M_s are observed. Contours of variations in the velocity of Rayleigh waves.given by Pilant[1], particularly for 20 second wave periods, show characteristics which are very similar to the contours of upper mantle Q given here. If a correlation can be successfully established, further improvement in the discriminatory power of the m_b versus M_s trends at low magnitudes may be possible. Evernden[2] shows data which indicate that difficulty with the discriminant at these distances may be due to variations in body wave amplitudes - the reasons and characteristics for such variations are given in the contours.

More accurate predictability of amplitude variations within a continental region by this method, beyond applications in more academic pursuits of deriving a model for the earth's interior, also provides a more reasonable method for predicting the detection capabilities of a seismic system observing signals at less than teleseismic distances.than does a simple amplitude-distance function for all distances and azimuths. Application of discriminants is not possible unless the signals used are detectable - prediction of this capability is obviously important to the problem.

1 Pilant, W. L. (1967), Final Technical Report, Tectonic features of the earth's crust and upper mantle; Office of Aerospace Research, Contract No. AF 49(638)-1534

2 Evernden, J. F., and J. Filson (1971), Regional dependence of Surface-wave versus body-wave magnitudes; J. Geophys. Res., 76, 3303-3308

2. A BRIEF REVIEW OF SEISMIC WAVE ABSORPTION

The absorption of energy carried by seismic waves through the earth has been of interest to science for quite some time, since the absorption represents departures of earth materials from perfect elasticity in the sense of Hooke's Law. These departures, in turn, reflect the strength and other elastic properties which influence the mobility of rock masses in the interior of the earth. As early as 1906, Nagoka made comment upon the absorptive properties of the earth based upon observations of seismic surface wave dispersion. Many similar reports have followed, and among the more important to the subject here are those by Gutenberg (1924) in a study of amplitude absorption in the upper mantle and crust using long-period Love waves and Jeffries (1929, 1931) in attempting to understand the mechanical characteristics in regions near the core-mantle boundary using seismic body waves. Birch and Bancroft (1938) published important results shown in laboratory studies of longitudinal wave attenuation in granite. Birch (1942) summarized state-of-the-art knowledge in seismic absorption and listed values of attenuation factors available at that time. Byerly (1942) briefly discussed the characteristics of internal friction in the earth, in essence rejecting the possibility of extension of a large body of theoretical work in fluid viscosity into solids as workable mechanisms for seismic attenuation. Gutenberg's 1945 estimates of attenuation in the mantle from observations of long-period surface waves and relatively long-period body waves (T = 4 sec) added to a growing body of attenuation factors. Bullen's text (1947) treated the problem of anelasticity in mathematical form following basic elasticity theory. Comprehensive surveys of seismic attenuation factors within the earth are given by Gutenberg (1951), Knopoff (1964), and Jackson and Anderson (1970). Additional references appropriate to specific aspects of Q are given within the text of this study at appropriate places.

3. Q IN A HOMOGENEOUS MEDIUM

Most of us are familiar with the phenomenon of damped oscillatory motions, where the amplitude of the oscillations gradually decrease with time to some infinitesimal value. The factor reflecting the amplitude decay is usually a constant, attenuating the amplitude of each successive increment of oscillation at a steady rate according to the mechanical characteristics of the vibratory system. Such mechanical damping is also observed in the amplitude of propagating seismic waves. The study of this absorption of dynamical energy in a propagation path provides one tool for estimating the physical characteristics of regions within the earth. Seismologists commonly express the absorption in terms of a dimensionless constant Q which reflects the minute amplitude loss in each cycle of motion caused by imperfect elasticity, or "anelasticity", in the medium through which the seismic waves moves. A higher value of Q indicates a medium which decreases the amplitude less than a medium with lower Q.

Amplitude decays of the kinds discussed above are observed to follow some exponential law which relates the amplitude A observed at some distance D (or time t x velocity v) to the original amplitude A_o by:

$$A = A_o e^{-kD} \tag{1}$$

where k is the amplitude absorption coefficient or damping factor. Birch (1942) and Gutenberg (1951) find that the relationship

$$k = \frac{\pi f}{QV} \tag{2}$$

satisfies the seismic data (f = frequency, V = wave velocity). Knopoff (1956) in a theoretical extension of Ricker's (1949) study of seismic pulse propagation in solids, finds

$$k = \frac{|\omega|}{2QV} \qquad\qquad (3)$$

The relationship applies to sinusoidal plane waves with small losses per wave cycle propagating in a homogeneous medium. Since sinusoidal motion is assumed, the angular frequency ω is equivalent to $2\pi f$, so relationships (2) and (3) are equivalent. This equality between the absorption coefficient k and seismic Q is widely used in the basic description of seismic wave amplitude attenuation (see Kolsky, 1953; Ewing, Jardetsky, and Press, 1956; Gutenberg, 1959, and others). The main mechanism of seismic energy loss is usually accepted to be one of kinetic energy converting to heat along the path of propagation. Reflections, scattering, or seismic mode conversions are not included in the basic assumption of an infinite homogeneous medium.

Several methods of determining Q from seismic data are available. Among the most commonly used in recent investigations is the method of spectral analysis of the seismic signal which permits a measure of the relative power present in the signal at several wave frequencies. If the source event is assumed to generate equal amplitude at all frequencies of interest and the wave path is considered non-dispersive (i.e., wave velocity is not a function of wave frequency), the relative power observed at different frequencies reflects absorptive path qualities since the higher frequencies will have experienced more wave cycles than lower frequencies for a given path. This approach requires a careful selection of signals for analysis to avoid noise contamination as well as the availability of computer facilities for spectral determinations with sufficient resolution to provide useful results.

Among other methods, Q may be determined from the logarithmic decrement of the signal δ (the logarithmic decrement is the time of wave propagation required for the original signal amplitude

at a given frequency to decrease by a factor of e^{-1}) through the simple relationship $Q = \frac{\delta}{\pi}$. Q is also defined by $Q = 1/\tan \phi$, where ϕ is the phase lag of strain in relation to applied stress in a cyclically stressed body.

Whether determined in the laboratory or from observations of data taken in paths of continental or even world-wide dimensions, these methods of determination require data or conditions which are not always available to those interested in examining absorptive properties within the earth. A simple method for determining absorption is described and applied in this work which alleviates this difficulty to some extent. With a reasonably controlled extrapolation of the results, it is also possible to extend Q found by the method into an estimate of absorptive characteristics in the upper mantle in lateral contour form -- a result not yet attempted in the more detailed and time consuming alternatives.

4. Q DETERMINED FROM PN

An application of equation (1), or equation (1) with equation (2), provides a relationship useful in the study of plane wave absorption in an infinite homogeneous medium. The seismic wave used in this study, however, requires a change in the assumption of infinite homogeneous conditions in order that the wave exist at all. That change is assumed here to be the boundary between the earth's crust and it's uppermost mantle commonly referred to as the Mohorovicic Discontinuity, or simply the "Moho". Observation of seismic signals shows that a compressional wave known as Pn propagates in the neighborhood of the Moho, supposedly generated by waves impinging on the interface between the crust and mantle materials. The spreading of energy over a curved wave front propagating away from the source region in the Pn wave must be accounte. for in order that absorption may be determined.

Based upon theory given by Heelan (1956), Pn propagates as a head wave in the uppermost mantle as shown in Figure 1. The figure gives a model of the structure and wave paths of interest to the problem. Heelan's ray theory was extended to wave theory by Brekhoviskikh (1960) and Grant and West (1965). In either approach, the head wave propagates in the higher velocity material along a path closely paralleling an interface between two materials with differing elastic parameters. Pn and the head wave are assumed to be the same mode of seismic energy propagation for this study.

The upper section of the model in Figure 1 represents the continental crust in this instance, with an average plane wave propagation velocity V_1 for wave paths of length L_o and L_1. Materials below are the uppermost mantle with a mean velocity V_2 and head wave path L parallel to the boundary and wholly within the mantle materials. θ is the critical angle determined by the velocities of the two media. The total wave path $L_o LL_1$ corresponds to the path $P_1 P_2 P_1$ in Heelan's original definition. The quantity r
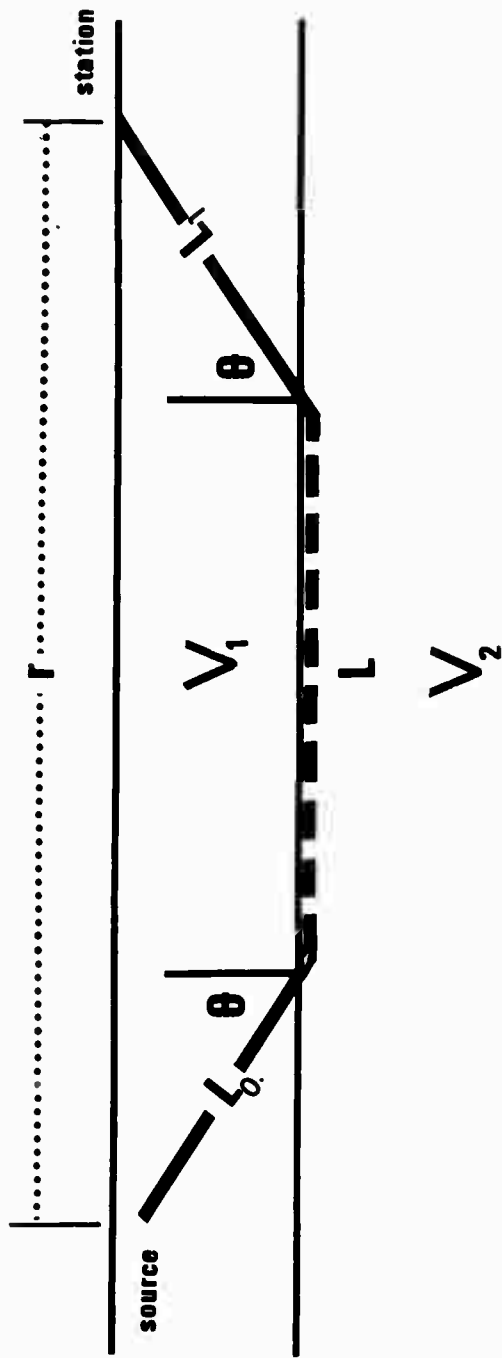
Figure 1. Head wave path model for Pn (after Grant and West). Main Pn path L with wave velocity V_2 in the upper mantle.

in the figure is the distance measured at the earth's surface between the source and receiver, or the epicentral distance.

Solutions to the problem of estimating the amplitude change in the head wave for the total path are of the form

$$A(r) = \frac{F(A_O)\ F(\theta,V)}{r^{1/2}L^{3/2}} \tag{4}$$

which simply states that the amplitude expected at some distance r from the source A(r) is proportional to the product of amplitude at the source $f(A_o)$ and an energy transfer function at the boundary $F(\theta,V)$, with the result reduced by some geometrical spreading factor related to the path length of the head wave L and total distance r. Additional terms for wave frequency and the shorter path lengths L_o and L_1 may be added for extension to wave theory and complete path considerations.

The factor of interest in (4) is the geometrical term in the denominator which provides the theoretical estimate of amplitude decrease related to the spreading of seismic energy in the head wave over an ever increasing area as the wave propagates away from the source region. For distances at which the head wave was observed in the data of this study (from about 200 to 2000 kilometers), the head wave path length L is approximately the same as the epicentral distance r, and the denominator in (4) is approximated by r^2. Distance D in (1) is the equivalent of r. Amplitude of the head wave is then expected to decrease at a rate proportional to the inverse square of distance from the source. Wave paths L_o and L_1, the critical angle, and any frequency effects are assumed to be essentially the same for all observations, and therefore not of importance to the determination of Q. Some further discussion about the influence of these factors is given later.

With the simplifying assumptions above, a combination of (1), (2), and the spreading factor r^{-2} results in the basic relationship needed for determination of Q from the Pn amplitude:

$$A = A_o r^{-2} e^{- \frac{\pi f r}{Q V}} \tag{5}$$

However, the A_o term is not available to us, since it represents the amplitude of the head wave at the point of generation in the crust-mantle boundary. A different form of (5) may be developed rather simply to eliminate the need for A_o in the following way. If A_1 is the amplitude of Pn at some distance r_1 from the source with an observed onset time of t_1, and A_2, r_2, t_2 are the same factors at some station further along a radial path with respect to the source, the relationship may be written

$$\frac{A_2}{A_1} = \left(\frac{r_1}{r_2} \right)^2 e^{- \frac{\pi f (t_2 - t_1)}{Q}} \tag{6}$$

Here it is assumed that the difference in arrival times $(t_2 - t_1)$ is an adequate representation of the distance between stations $(r_2 - r_1)$ divided by the average velocity V between them. Wave frequency is estimated as the average frequency observed at stations 1 and 2.

Certain variations to the simple scheme are possible, and among those used is the idea that the average Q determined for a head wave path L is the sum of possibly different Q along path segments of different lengths. That is, if Q_i is the Q for path segment l_i $(i = 1, 2, 3, \cdots, n)$, then

$$
\begin{aligned}
Q_{path} &= Q_1 \frac{l_1}{L} + Q_2 \frac{l_2}{L} + Q_3 \frac{l_3}{L} + \ldots + Q_n \frac{l_n}{L} \\
&= \sum_{i=1}^{n} Q_i \frac{l_i}{L}
\end{aligned} \tag{7}
$$

This approach allows an estimate of Q for path segments which were
not observed in sequence from the same source event or where very
strong crustal amplitude influences at one observation point con-
tradict general results in some region. It also provides a
method for comparing the reliability of estimates made from the
signals of different sources where the observational data do not
include the same station pairs. Where such estimates are made,
the estimated Q values are enclosed in parenthesis throughout
this report.

Equations (6) and (7) are the relationships used to determine
upper mantle Q from measurements of the Pn head wave for paths
beneath the United States presented in this study. However,
certain basic assumptions beyond those mentioned above are also
important for understanding several factors which are both
general and unique to determination of Q from the Pn phase.
These factors are discussed in some detail below.

5. SOME ASSUMPTIONS ABOUT Q AND Q FROM PN

In determining Q for the upper mantle beneath the United States from the Pn wave, it is assumed Pn propagates everywhere in the uppermost mantle as a head wave and that the velocity of the wave is constant between the stations where the amplitude data were obtained. It is evident in the data here that several important interfaces and velocities may be present in some instances, but by carefully observing the amplitude trends, the arrivals from each may be identified and an appropriate Q can be calculated.

As a reflection of the velocity differences, epicentral distance is critical, especially for observations in the western United States. The possibility of a layer of low velocity material in the upper mantle beneath parts of this region has been suspected for quite some time (see Gutenberg, 1948). As detailed by Evernden (1967), Pn signals in that region follow a velocity on the order of 7.9 kilometers/second to distances of about 800 - 1000 kilometers. At greater distance, the first plane wave signal seen is from a Pn which apparently propagates at a velocity on the order of 8.2 kilometers/second or greater, and this wave may follow a boundary some depth below the low velocity materials. If the source event is in the eastern United States and the wave is observed in either the eastern or western region, the higher velocity wave is usually observed. Among other observations, this suggests that a higher velocity layer may be present beneath the low velocity zone in the west. Q values calculated here support such a possibility since different values of Q were found for a single path if the source events were located at distances which would produce waves from both media.

Frequency independence of Q is assumed here since there is little absolute evidence to the contrary. In many models of the possible attenuation processes, some dependence of Q upon the frequency of the waves is indicated mathematically, with higher

frequencies attenuated more than lower frequencies. Knopoff (1964) observed that no frequency dependence is indicated over many octaves of frequency in single crystals and metals. Kanamori (1967, a,b) demonstrated that upper mantle Q determined from short-period (about 1.0 second) body wave reflections from the earth's core indicate about the same value of Q as that obtained by Anderson and Archambeau (1964) in an estimation of Q for the upper mantle using long-period (50 - 300 second) surface waves. Jackson and Anderson (1970) also take this position, and while frequency dependent Q may be discussed (Solomon and Toksoz, 1970; Archambeau, et al., 1969), that dependence has not been established with sufficient confidence to warrant consideration in the Pn data because of it's limited frequency band (5.0 to 0.7 Hertz in this study).

There is also some possibility that the crustal paths may contribute some amplitude amplification or attenuation, but this is considered to be insignificant in the results given. Contributions to Q from the crustal path would lie primarily in the leg beneath the receiving stations (L_1) since the path to the mantle in the source region is common to the observations. In any case, Q for the crust may be greater than that for the upper mantle (Archambeau, et al., ranging from 200 to almost 1000 (Press, 1964; Anderson and Archambeau; Kanamori; Sutton, et al., 1968; Hill, 1970), while upper mantle values are more on the order of 100 (Anderson and Archambeau, Knopoff) to about 500 (Dorman, 1968; Archambeau, et al., Pasechnik (1970) notes a close correspondence in Q values obtained from spectral ratios (another Q determination method) and amplitude procedures, and finds Q in the upper mantle from Pn amplitude measurements ranging from 210 - 570. The spreading factor and location of the observations are not given in his description. These data disagree with Teng's (1968) estimate of an average Q in the upper mantle above 950 kilometers of about 93, but Teng himself identified the need for additional

data points in his result. The higher crustal Q's should, there-
fore, not depress mantle Q determinations, and the very short
crustal paths relative to the head wave path lengths are not
likely to increase the Q determinations to any great extent.

The problem of possible unequal azimuthal radiation of Pn
energy from the source is not likely to be an influence on the
results here since every effort is made to obtain the Q estimate
from stations which are as near "in-line" as practically possible.
Some differential azimuth data are included, but these results
are used only where they do not disagree with short in-line Q
estimates. Sutton, et al., also note that crustal path wave
amplitudes from small magnitude earthquakes (in the range used
here) showed no strong azimuthal effects not seen in crustal wave
amplitudes from explosive sources. This condition applied even
though the source events occurred within the crust itself.

6. DATA BASE AND PROCEDURES

Pn traveltime, wave period, and wave amplitude data for determining upper mantle Q were obtained from 16- and 32-mm film seismograms recorded by the short-period seismograms of Long Range Seismic Measurement (LRSM) mobile laboratories and permanent observatories of the VELA Uniform Program. Station identifiers and the location of observation points are given in Table I. The signals recorded by these systems from the earthquakes and underground explosions given in Table II were measured from X10 magnification of the seismograms, converted to ground motion (zero-to-peak) through appropriate system response calibrations, and entered into equation (6) for determination of the Q for paths between two observation points. Care was taken to obtain amplitude measurements in the first cycle of discernible motion in the Pn signal to avoid ambiguity in the results. Data for several explosions were taken from published reports which provide detailed measurements, and a cursory check of these data was also made to insure accuracy and completeness.

TABLE I

Station designators and nearby towns and cities for stations
recording seismograms used as a data source.

APOK	Apache, Oklahoma
ATNV	Austin, Nevada
AXAL	Alexander City, Alabama
AYSD	Academy, South Dakota
AZTX	Amarillo, Texas
BLWV	Beckley, West Virginia
BPCL	Bishop, California
BRPA	Berlin, Pennsylvania
BSMA	Billings, Montana
BXUT	Blanding, Utah
CPCL	Compo, California
CQNV	Caliente, Nevada
CRNB	Crete, Nebraska
CUNV	Currant, Nevada
DHNY	Delhi, New York
DRCO	Durango, Colorado
DUOK	Durant, Oklahoma
EBMT	East Braintree, Manitoba
EKNV	Eureka, Nevada
EUAL	Eutaw, Alabama
EYNV	Ely, Nevada
FMUT	Fillmore, Utah
FOTX	Fort Stockton, Texas
FRMA	Fronnie, Montana
FSAZ	Flagstaff, Arizona
GEAZ	Globe, Arizona
GIMA	Glendive, Montana
GPMN	Grand Rapids, Minnesota
GVTX	Grapevine, Texas
HBOK	Hobart, Oklahoma
HDPA	Howard, Pennsylvania
HETX	Hempstead, Texas
HHND	Hannah, North Dakota
HXWY	Hawk Springs, Wyoming
HLID	Hailey, Idaho
HVMA	Havre, Montana

TABLE I (continued)

JELA	Jena, Louisiana
JPAT	Jasper, Alberta
JRAZ	Jerome, Arizona
JUTX	Juno, Texas
KCMO	Kansas City, Missouri
KGAZ	Kingman, Arizona
KMCL	Kramer, California
KNUT	Konab, Utah
LAO	Subarray Ao, Montana
LCNM	Las Cruces, New Mexico
LGAZ	Long Valley, Arizona
LNMA	Lewistown, Montana
LSNH	Lisbon, New Hampshire
MNNV	Mina, Nevada
MPAR	Mountain Pine, Arkansas
MVCL	Marysville, California
NDCL	Needles, California
NLAZ	Nazlini, Arizona
PGBC	Prince George, British Columbia
PHWA	Pomeroy, Washington
PMWY	Pole Mountain, Wyoming
PQID	Preston, Idaho
PTOR	Pendleton, Oregon
RYSD	Redig, South Dakota
RKON	Red Lake, Ontario
RTNM	Raton, New Mexico
RYND	Ryder, North Dakota
SEMN	Sleepy Eye, Minnesota
SGAZ	Springerville, Arizona
SJTX	San Jose, Texas
SKTX	Shamrock, Texas
SNAZ	Sunflower, Arizona
SROR	Sparta, Oregon
SSTX	Sanderson, Texas
SVAZ	Springerville, Arizona
SWMA	Sweetgrass, Montana
TDNM	Tres Piedras, New Mexico
TFCL	Taft, California
TKWA	Tonasket, Washington
TLWY	Thermopolis, Wyoming

TABLE I (continued)

VOIO	Vinton, Iowa
WFMN	Wykoff, Minnesota
WINV	Winnemucca, Nevada
WNSD	Winner, South Dakota
WOAZ	Winslow, Arizona
WZNV	Warm Springs, Nevada
BMSO	Blue Mountains Observatory, Oregon
CPSO	Cumberland Plateau Observatory, Tennessee
TFSO	Tonto Forest Observatory, Arizona
UBSO	Uintah Basin Observatory, Utah
WMSO	Wichita Mountains Observatory, Oklahoma

TABLE II

Earthquakes and explosions (capitalized) used in determination of upper mantle Q variations

Source Name	Date	Time (Z)	Lat.	Long.	Depth	m_b
Washington-Oregon Border	6 Nov 62	03:36:47	45.8N	122.5W	44	4.95
Off Oregon Coast	7 Jul 64	13:44:40	43.4N	127.2W	7	5.7
Del Norte, California	23 Aug 62	19:29:16	41.8N	124.1W	33	4.95
Monterey, California	14 Sep 63	19:46:16	36.7N	121.8W	15	4.44
Southern California	1 Jan 65	08:04:16	34.0N	117.6W	14	4.64
California-Nevada Border	23 Oct 64	13:56:11	38.5N	118.4W	26	3.67
Bridgeport, California	5 Apr 62	21:27:54	38.6N	119.3W	25	3.03
Fallon, Nevada	20 Jul 62	09:02:08	39.6N	118.2W	20	4.4
Northern New Mexico	23 Jan 66	01:56:12	36.5N	104.3W	33	4.95
Northern New Mexico	6 Jun 63	08:05:36	36.5N	104.3W	33	3.19
Arizona	11 Sep 63	11:59:41	33.2N	110.7W	33	3.88
Arizona-Mexico Border	25 Dec 64	14:09:48	32.3N	113.7W	33	3.23
Cache Creek, Utah	5 Sep 62	16:04:29	40.7N	112.0W	14	4.1
Western Montana	26 Jun 64	12:24:29	48.2N	115.1W	33	3.59
Hebgen Lake, Montana	25 Feb 62	17:17:39	45.2N	111.2W	25	5.07
Hebgen Lake, Montana	21 Oct 65	19:35:02	44.8N	111.0W	33	3.92
Utah "Rockburst"	6 Jun 64	06:44:32	39.5N	110.3W	31	3.74
Wyoming	3 Jun 65	19:30:26	43.6N	106.5W	33	3.78
Nebraska-South Dakota	28 Mar 64	10:08:43	43.0N	101.6W	16	3.21
Texas-Louisiana Border	24 Apr 64	07:33:54	31.5N	93.9W	33	3.21
"	28 Apr 64	00:30:46	"	"	"	3.79
"	28 Apr 64	21:18:35	"	"	"	3.59
"	3 Jun 64	02:27:27	"	"	"	3.63
Poplar Bluff, Missouri	3 Mar 63	17:30:13	36.7N	90.1W	18	4.5
New Madrid, Missouri	2 Feb 62	06:43:31	36.5N	89.6W	15	4.7

TABLE II (continued)

Source Name	Date	Time (Z)	Lat.	Long.	Depth	m_b
Missouri	6 Mar 65	21:08:50	37.4N	91.1W	18	4.10
Georgia-Alabama Border	18 Feb 64	09:31:12	34.7N	85.4W	33	3.62
Tennessee	19 Dec 65	22:19:10	35.9N	89.9W	5	3.84
West Virginia	25 Nov 64	02:50:07	37.4N	81.7W	33	3.59
ROCKVILLE DAM (Colorado)	3 Apr 66	16:21:34	37.4N	106.2W	0	3.70
CLIMAX MOLYEBDENUM	23 May 64	21:44:59	37.6N	106.3W	0	3.82
RUILSON (Colorado)	10 Sep 69	21:00:00	39.4N	107.9W	3	4.62
GASBUGGY (New Mexico)	10 Dec 67	19:30:00	36.7N	107.2W	1	4.72
SHOAL (Nevada)	26 Oct 63	17:00:00	39.2N	118.4W	0	4.62
AARDVARK (NTS)	12 May 62	19:00:00	37.1N	116.0W	0	4.55
HARDHAT (NTS)	15 Feb 62	18:00:00	37.2N	116.1W	0	4.15
FORE (NTS)	16 Jan 64	16:00:00	37.1N	116.0W	0	4.85
TAN (NTS)	3 Jun 66	14:00:00	37.1N	116.1W	1	4.50
STONES (NTS)	22 May 63	15:40:00	37.1N	116.0W	0	4.90
SALMON (Mississippi)	22 Oct 64	16:00:00	31.1N	89.6W	1	4.27

7. PRELIMINARY RESULTS OF UPPER MANTLE Q DETERMINATION

7.1 Path Results and Tentative Contours of Upper Mantle Q

Results of Q determinations between stations observing the Pn wave are shown in Figure 2 for high velocity Pn paths and in Figure 3 for paths with lower Pn velocity in the west. The results are also tabulated in Table III. No difference in Q is noted which might be related to explosive or earthquake source type, as expected.

In Figures 2 and 3, paths for which Q has been determined are indicated by straight lines which are radial to the particular source event, beginning with a short hack perpendicular to the radial path at the distance of the station where the A_1 value was measured and terminating the station location where A_2 was obtained. The numerical value on the line is the value of Q calculated for the path. Values in parenthesis were estimated according to the relationship given in equation (7). Several events, in particular earthquake sources, provided only one or two paths which were useful because of distance, azimuth, or signal readability restrictions. All paths for which Q was determined are not plotted because of space limitations (they are given in Table III), but those which are plotted are representative for the path or area.

Figure 4 is an interpretation of the calculated Q for paths in the 8.2 kilometer/second velocity upper mantle as contours of Q at multiples of 250 up to Q = 1000. A more detailed contouring interval is not considered justified because of the necessity of subjectively judging the areal extent represented by a single path determination and the estimated reliability of the determination as discussed below. For instance, the great majority of paths crossing the central United States have a calculated Q of over 1000, but in some cases, Q as low as 200 are indicated. Since some variations may easily represent unique and very localized paths or anamolous observations, the contours are strongly influenced by the Q determined from typical paths in the region, rather
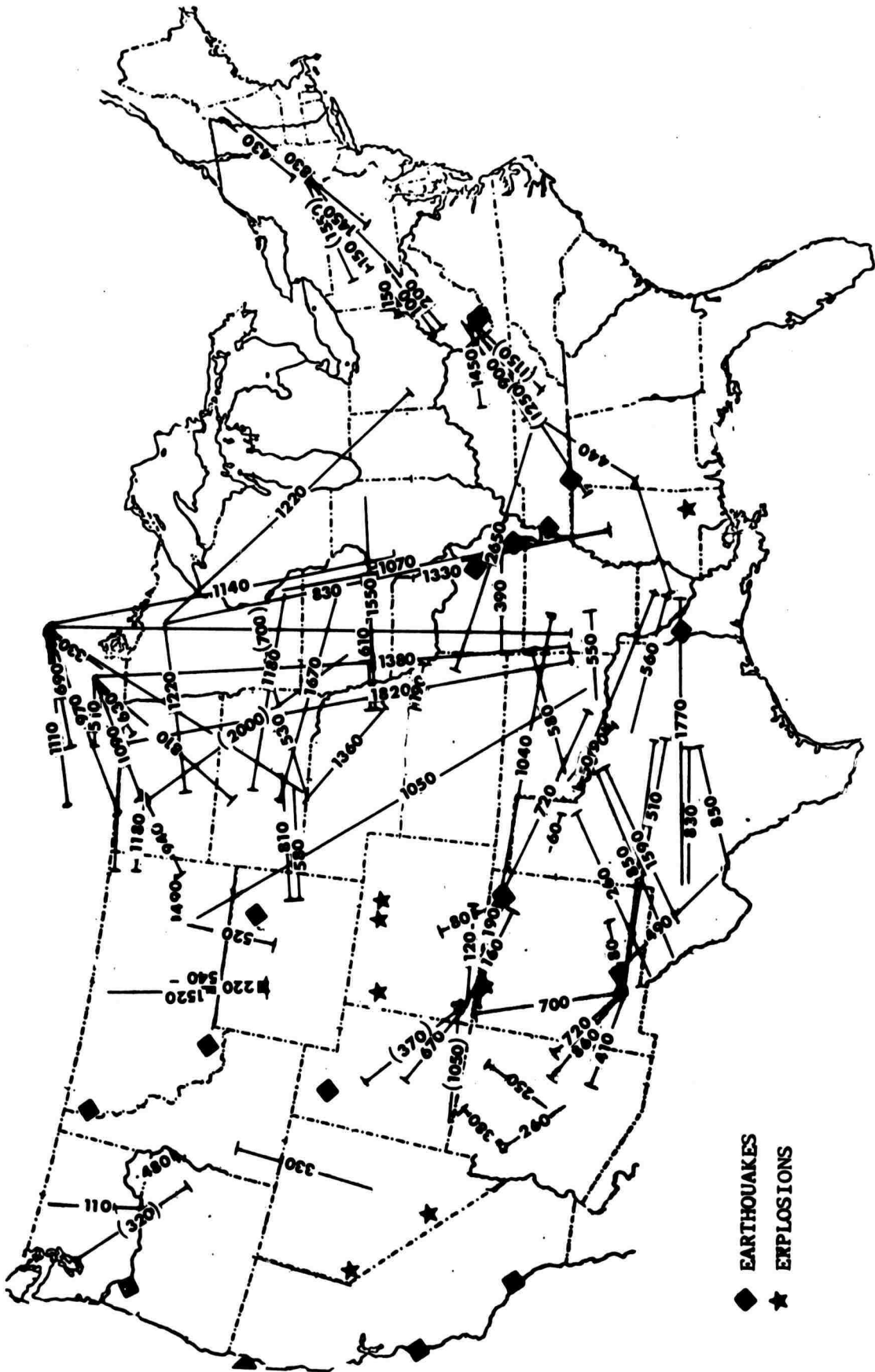
Figure 2. Upper mantle Q for selected Pn paths with velocity 8.2 km/sec. or greater. Paths begin at short hack and terminate at station observing A₂ (see text). Complete path data given in Table III.

EARTHQUAKES
EXPLOSIONS

Figure 3. Upper mantle Q for selected Pn paths with velocity of about 7.9 Km/sec. Paths begin at short hack and terminate at station observing A_2 (see text). Complete patn data given in Table III.

TABLE III

Upper mantle Q determined from Pn amplitudes listed by source event, stations beginning and terminating path, and high* (8.2 km/sec or greater) or low (about 7.9 km/sec).

VELOCITY PATHS IN THE MANTLE

Off Oregon Coast

FRMA-GIMA	490*
KNUT-DRCO	670*
SGAZ-SNAZ	260*
SGAZ-WOAZ	220*
JRAZ-WOAZ	20*

Washington-Oregon Border

FMUT-DRCO	(370)*
MVCL-TFCL	Hi Q*

Del Norte

DRCO-LCNM	720*
FMUT-DRCO	Hi Q*

Monterey

KNUT-BXUT	660*
DRCO-RTNM	160*
AZTX-SKTX	60*
FRMA-GIMA	Hi Q*
GIMA-RYND	940*

Southern California

WOAZ-LCNM	410*

California-Nevada Border

SGAZ-JRAZ	630
JRAZ-LGAZ	270
KNUT-DRCO	350
GEAZ-LCNM	860*
WOAZ-LCNM	860*

Bridgeport

WINV-HLID	250

Fallon

TNCL-CPCL	170
LCNM-SSTX	490*
PMWY-HKWY	Hi Q*
HKWY-WNSD	580*
HKWY-AYSD	810*
WNSD-AYSD	(1800)*

Northern New Mexico (2 events)

DRCO-FMUT	Hi Q*
WNSD-SEMN	Hi Q*
CRNB-KCMO	70*
KCMO-ENMO	390*
RGSD-RKON / WNSD	460*

Arizona

CUNV-MNNV	180
RTNM-AZTX	260
AZTX-SKTX	340

Arizona-Mexico Border

JRAZ-KNUT	340
WOAZ-DRCO	130
JRAZ-UBSO	950*

Cache Creek

HLID-PTOR	480
KNUT-FSAZ	170
KNUT-TFSO	60
SEMN-HTMN	(700)*
AYSD-SEMN	Hi Q*
HBOK-WMSO	50*
HBOK-CTOK	Hi Q*
HBOK-MPAR	Hi Q*

Western Montana

GIMA-RYND	1180*
GIMA-WNSD	Hi Q*
RYND-HHND	Hi Q*
RYND-RKON	1110
HHND-RKON	690*
HHND-EBMT	510*
GIMA-HHND	2670*
HLID-EKNV	330*

Hebgen Lake (2 events)

HLID-VTOR	Hi Q
HLID-PTOR	140
HLID-WINV	360
HLID-ATNV	350
ATNV-MNNV	160
FMUT-KNUT	650
RYND-RKON	970*
RYND-GPMN	1220*
RYND-WFMN	1180*
RYND-VOIO	1670*
SGAZ-LGAZ	90*
DRCO-RTNM	80*
DRCO-LCNM	700*

Utah "Rockburst"

EKNV-MNNV	260
DRCO-RTNM	60
KNUT-SGAZ	60
KNUT-WOAZ	150
KNUT-JRAZ	100
KNUT-LGAZ	200
KNUT-SNAZ	370

Wyoming

KNUT-SGAZ	380*
KNUT-JRAZ	250*

TABLE III (continued)

Nebraska-South Dakota Border

EBMT-RKON	330*

Poplar Bluff

MPAR-HBOK	580*
SSTX-LCNM	240*
CPSO-BLWV	1450*

New Madrid

RTNM-DRCO	120*
HBOK-EFTX	850*
GNNM-LCNM	80*
LCNM-TCNM	(400)*
HBOK-BMTX	1590*
RTNM-KNUT	680*
DRCO-KNUT	(1050)*
GNNM-SFAZ	390*
GNNM-FSAZ	690*

Texas-Louisiana (4 events)

EUAL-CPSO	Hi Q*
EUAL-BLWV	(1250)*
CPSO-BLWV	900*
BLWV-BRPA	100*
CPSO-BRPA	1460*
EUAL-BRPA	820*
	520*
GVTX-LCNM	1050*
	520*
	530*
	490*
GVTX-RTNM	330*
	260*
	250*
GVTX/JELA-EBMT	1670*
	1030*
	1450*
GVTX-JUTX	1050*
	750*
	730*
GVTX/JELA-RKON	1080*
	2870*
JELA-BRPA	2760*
GVTX-HHND	1820*
	(1820)*

Texas-Louisiana (continued)

JUTX-LCNM	280*
	370*
	360*
GVTX	
JELA-FRMA	1050*
GVTX/JELA-WMSO	90*

Missouri

VOIO-RYND	(2000)*
VOIO-RKON	930*
GVTX-FOTX	Hi Q*
GVTX-LCNM	260*
BLWV-BRPA	150*
BLWV-DHNY	1000*
BRPA-DHNY	(1550)*

Georgia-Alabama

JELA-DUOK	550*
BLWV-BRPA	280*
BRPA-DHNY	1450*
JELA-TRNM	1040*

Tennessee

CRNB-WNSD	1360*
KCM)-RKON	1140*

West Virginia

BRPA-HDPA	100*
DHNY-LSNH	430*
BRPA-LSNH	830*
BRPA-DHNY	(1450)*
CPSO	
BRPA-GPMN	1220*

SALMON (Mississippi)

EUAL-CPSO	440*
EUAL-BLWV	820*
CPSO-BLWV	(1150)*
BRPA-HDPA	150*
BRPA-DHNY	460*
JELA-VOIO	1330*
JELA-WFMN	1070*
JELA-GPMN	830*
WFMN-GPMN	160*
GVTX-LCNM	530*

SALMON (cont.)

GVTX-RTNM	720*
RTNM-DRCO	180*
JELA-GVTX	560*
JELA-FOTX	830*
GVTX-FOTX	1770*
JELA-WMSO	260*
FOTX-LCNM	250*
LCNM-DRCO	760*

SHOAL (Nevada)

WINV-HLID	110
WINV-BMSO	310
CUNV-UBSO	650
KNUT-BXUT	640
BXUT-DRCO	340
TDNM-RTNM	70*
RYND-EBMT	1090*
HHND-EBMT	630*
RYND-HHND	(1920)*

CLIMAX (Colorado)

UBSO-HLID	250
GIMA-EBMT	810*
DRCO-NLAZ	130

ROCKVILLE DAM (Colorado)

KNUT-TFSO	50
RGSD/WNSD-RKON	430*
CRNB-KCMO	190*
KCM)-CPSO	2650*

RUILSON (Colorado)

UBSO-BMSO	200
KNUT-TFSO	130
TFSO-TUC	200
CRNB-BYIO	660*
CRNB-WQIL	1550*
KNUT-BPCL	380

TABLE III (continued)

GASBUGGY (New Mexico)		UNDERGROUND EXPLOSIONS Nevada Test Site	
KNUT-CONV	160	SFAZ-SVAZ	50
CQNV-WZNV	100	SVAZ-MLNM	10
UBSO-PQID	190	MLNM-TCNM	(480)
UBSO-HLID	190	NDCL-CPCL	130
BMSO-PHWA	480	TNCL-CPCL	70
TLWY-BSMA	220*	MNNV-MVCL	160
TLWY-LAO	520*		180
TLWY-LNMA	540*	TCNM-LCNM	(530)
TLWT-HVMA	1520*	LCNM-GNNM	430
WNSD-RKON	410*		
PHWA-CCWA	160		
GMSO-CCWA	(320)*		

UNDERGROUND EXPLOSIONS Nevada Test Site	
ATNV-WINV	180
	100
WINV-VTOR	330
	490
PTOR-TKWA	170
	85
ATNV-HLID	90
	340
	170
WINV-HLID	210
WINV-BMSO	300
	360
EYNV-HLID	110
FMUT-VNUT	580
	(1130)
VNUT-PMWY	130
WNSD-SEMN	330*
	720*
SWMA-JPAT	1240*
CUNV-EKNV	290
KNUT-DRCO	180
	200
	260
KNUT-BXUT	330
BXUT-DRCO	210
DRCO-RTNM	170
	310
WMAZ-FSAZ	270
FSAZ-LCNM	120*
	520
FSAZ-SFAZ	160
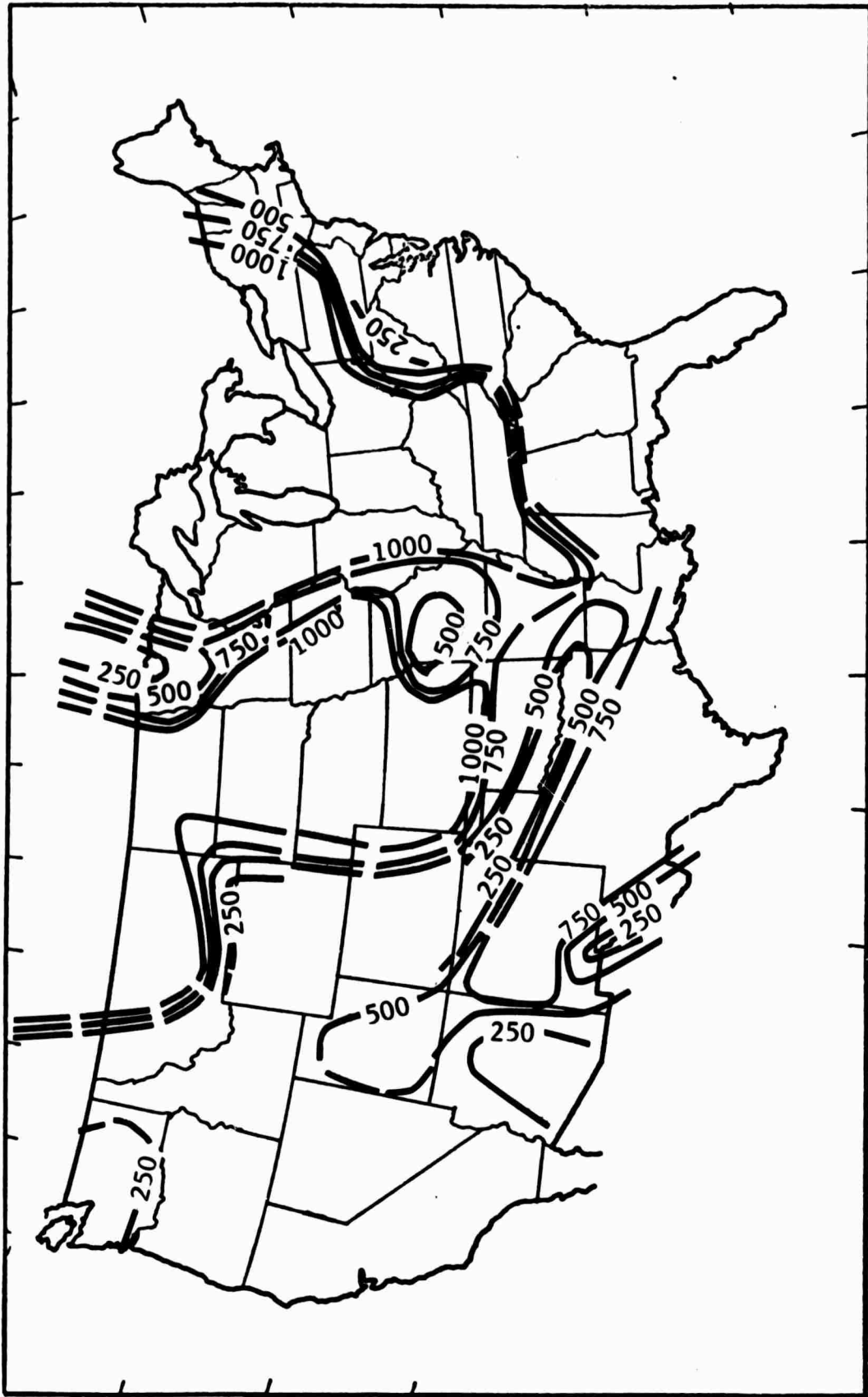
Figure 4. Contours of upper mantle Q from Pn paths with velocity of 8.2 km/sec. or greater

than by single observations of anamolous amplitudes. Q in the lower velocity materials in the western United States is given in Figure 5 with a contour interval of 100 beginning at Q = 150. Very high values of Q (up to Q = 950 in one instance) calculated for central Utah are not shown in the contours because of space limitations. Paths in the lower velocity are repeated more often in the data obtained, permitting the reduced contour interval.
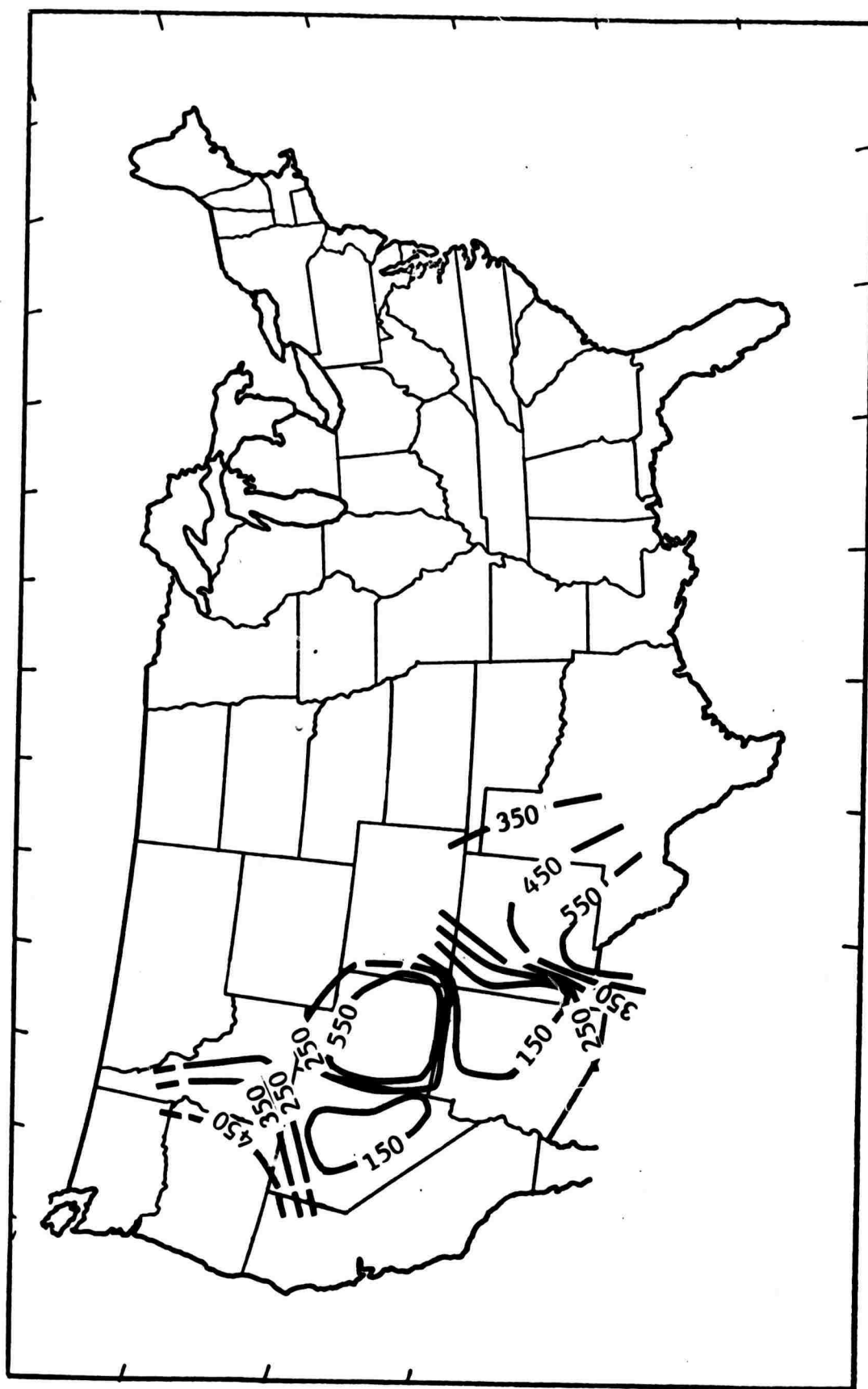
Figure 5. Countours of upper mantle Q from Pn paths with velocity of about 7.9 km/sec.

7.2 Reliability of the Q Estimate

Values of Q greater than about 1000 are not contoured in the
figures since they usually result from calculations in which
small decimals are found in the denominator of one of the terms
in equation 5. The denominator represents correction of the
amplitude for the spreading factor, and a slight change in the
logarithmic values, say 0.01 or 0.02 units, can double or halve
the Q values when attenuation is very low. Further, if a negative
logarithm appears in this position, an increase in amplitude with
distance is indicated. Such an increase is physically impossible,
and most likely represents unavoidable measurement error or inter-
ference effects where little attenuation is present. Very high
values of Q (over about 1000) and negative Q are simply assumed to
represent very low attenuation in the figures. Values of Q less
than about 1000 are not subject to this difficulty in the range
of observations here, and are therefore felt to be more depend-
able as accurate estimates of upper mantle Q.

While insufficient data were observed to provide a basis for
statistical estimate of Q variability for any of the paths, sev-
eral paths and major regions have results which clearly indicate
that the estimates are realistic. Some paths also include Q
determinations from signals which were obtained from events
positioned very nearly at 180° of azimuth from each other with
respect to the path of interest, in effect providing a "reversed
profile" for the Q determined. A few of these paths are listed
in Table IV from the data given in Table III for comparison. The
data sets for Texas-Louisiana earthquakes and Nevada Test Site
(NTS) explosions also provides the information needed to demon-
strate repeatibility from sources in the same source regions.

On a quantitative basis, the Q data are very repeatable along
a given path, with the range of observations seldom exceeding as
much as 50% of the mean value of the observations. Many paths
show considerably less variability, even in the higher Q values

TABLE IV

Selected paths showing repeatibility of upper mantle Q in both
high* and low velocity Pn paths from several sources.

Path Between Stations		Upper Mantle Q	Source Event
DRCO	LCNM	700*	Hebgen Lake
		720*	Del Norte
		760*	SALMON
WINV	BMSO	310	SHOAL
		300	FORE
		360	STONES
CRNB	KCMO	190*	ROCKVILLE DAM
		220*	Tennessee
		70*	Northern New Mexico
GVTX	RTNM	330	Texas-Louisiana
		260	Texas-Louisiana
		250	Texas-Louisiana
KNUT	DRCO	260	AARDVARK
		200	STONES
		180	HARDHAT
		260	FORE
		530 $^{(*)}$	SHOAL
		670*	Off Oregon Coast
GVTX JELA	EBMT	1670*	Texas-Louisiana
		1030*	Texas-Louisiana
		1450*	Texas-Louisiana

where Q estimates might be somewhat less reliable because of the small number problem. The 50% range applies to paths repeated from the same source, from slightly different sources, from estimation according to (7), and from "reversed profile" observations. Regional data reflect the reliability, with regions where low Q is observed remaining consistently low for the great majority of observations, and regions of High Q consistently high or estimated as high because of negative Q results.

7.3 An Application and Further Test of Upper Mantle Q

If the values of Q contoured in Figures 4 and 5 have much
meaning, it should be possible to estimate the average Q for
various paths and use the average Q as a means of estimating Pn
amplitude independently. By observing the amplitude and any
particular location, it should then be possible to predict Pn
amplitude at other locations by applying the amplitude attenua-
tion calculated from path segments with attenuative properties
indicated by the values of Q. Such a test is shown below for Pn
amplitudes observed from the underground nuclear explosion SHOAL
which was detonated in western Nevada. Some data from this
source were used in developing the Q contours, but over one-half
of the data from the stations recording Pn waves could not be
used because of distance or azimuth limitations. The comparison
of amplitudes predicted from application of the Q given in
Figures 4 and 5 along paths to these stations, particularly the
unused stations, should be a valid test of how useful the estim-
ate of upper mantle Q can be.

Original signal measurement data for the Pn wave from SHOAL
are given in Table V. Data here show that some very strong
azimuthal function is operating in the signal distribution for
this particular event, with nearly an order of magnitude range
in amplitude observed at several stations about equidistant, but
at different azimuths, from the source. It is therefore neces-
sary to examine the data with some control upon azimuth, and this
is the single restriction used in testing the Q. Comparison of
station amplitudes below is undertaken in azimuthal sectors,
rather than without regard to azimuth, as would be the typical
case.

The method used is as follows:
(1) average Q for the path from SHOAL to each station was obtained
by estimating the percentage of the total path in the Q values
given in Figures 4 and 5 and summing according to equation (7);

(2) the exponential term of equation (5) was then calculated and
multiplied by r^{-2}, giving a factor amounting to the reduction in
amplitude of the A_0 term expected for the path considered; and
(3) the ratio of amplitude reduction for stations within azimuthal
sectors was computed from the original observations, and the same
ratio was computed for the predicted amplitude reduction for a
comparison. The result of the various steps is given in Table VI
for steps (1) and (2) and in Table VII for the third step com-
paring the observed and predicted amplitude ratios. The amplitude
at the station closest to SHOAL was used as the normalizing term
for each azimuthal sector in the results shown in Table VII.

Comparison of the predicted and observed amplitude ratios to
the north of SHOAL show very good agreement, reflecting the
number of paths from which the Q was originally calculated. The
first three stations of the north profile are assumed to have
detected a signal from the higher velocity materials. The
consistency between the two results was not entirely expected,
since not very much direct information of high velocity Q was
available for a major part of the path (Q = 300 was assumed for
the factor in the high velocity materials under Nevada throughout
this comparison).

Ratios northeast of SHOAL comparing WINV, RYND, and HHND are
considered very poor, with the predicted amplitudes far below the
observed values. No information upon high velocity Q beneath
Idaho and western Wyoming was available in the original data, and
the difficulty may lie in greatly underestimated Q for that region.
An average Q for the path would have to be on the order of Q
= 1200 to satisfy the amplitudes observed. This is not an entire-
ly unreasonable value, since the calculated Q of (1920) was
indicated by SHOAL signals (see Table III) for the path between
RYND and HHND, leaving the original estimate of Q = 300 beneath
Idaho and Wyoming paths in reasonably good stead.

TABLE V

Pn data from stations recording signals from the SHOAL explosion

Station	Distance (km)	Traveltime (sec)	Wave Period (sec)	Wave Amplitude (millimicrons)
EKNV	231	35	0.5	1445
W1NV	251	38	0.8	467
MVCL	252	38	0.4	272
CUNV	260	39	0.4	1264
KNUT	544	75	0.5	28
HLID	602	82	0.4	11
BMSO	633	98	0.5	30
CPCL	741	100	0.4	15
UBSO	765	106	0.4	8.4
BXUT	802	108	0.5	13
TFSO	837	113	0.5	13
DRCO	946	126	0.6	5.4
TKWA	1071	143	0.6	4.5
TDNM	1109	148	0.8	5.4
RTNM	1261	168	0.8	2.2
LCNM	1303	174	1.0	10.5
AZTX	1515	198	0.8	8.4
SKTX	1662	217	1.0	8.0
RYND	1678	222	0.5	47.5
WMSO	1827	235	0.7	4.3
APOK	1836	235	0.8	(14)
HHND	1905	243	0.8	55

TABLE VI

Estimated average Q for Pn paths from SHOAL and calculated reduction in initial wave amplitude expected from Q_{path}.

Station	Percent of total path	Estimated Q	Contribution to Q_{path}	Initial amplitude (A_o) reduction
EKNV	100	150	Q_{path} = 150	0.437
WINV	100	150	Q_{path} = 150	0.660
MVCL	100	170	Q_{path} = 170	0.246
CUNV	90	150	135	
	10	250	25	
			Q_{path} = 160	0.218
KNUT	80	150	120	
	10	250	25	
	10	350	35	
			Q_{path} = 180	0.0025
HLID	50	150	75	
	50	250	125	
			Q_{path} = 200	0.0110
BMSO	20	150	30	
	20	250	50	
	20	350	70	
	40	450	180	
			Q_{path} = 330	0.0390
UBSO	50	150	75	
	20	250	50	
	30	500	150	
			Q_{path} = 275	0.0080
BXUT	60	150	90	
	10	250	25	
	30	650	195	
			Q_{path} = 310	0.0180
TFSO	100	150	Q_{path} = 150	0.0013
DRCO	50	150	75	
	10	250	25	
	30	650	195	
	10	150	15	
			Q_{path} = 330	0.0150

TABLE VI (continued)

Station	Percent of total path	Estimated Q	Contribution to Q_{path}	Initial amplitude (A_o) reduction
TKWA	80	300	240	
	20	200	40	
			Q_{path} = 280	0.0060
TDNM	40	300	120	
	40	500	200	
	20	150	30	
			Q_{path} = 350	0.0150
RTNM	30	300	90	
	40	500	200	
	30	200	60	
			Q_{path} = 350	0.0090
LCNM	50	300	150	
	10	250	25	
	30	600	180	
	10	400	40	
			Q_{path} = 395	0.0150
AZTX	30	300	90	
	60	500	300	
	10	200	20	
			Q_{path} = 410	0.0095
SKTX	30	300	90	
	50	500	250	
	20	200	40	
			Q_{path} = 380	0.0069
RYND	60	300	180	
	40	750	300	
			Q_{path} = 480	0.0200
WMSO	30	300	90	
	30	500	150	
	40	100	40	
			Q_{path} = 280	0.0060
APOX	30	300	90	
	30	500	150	
	40	100	40	
			Q_{path} = 280	0.0024
HHND	50	300	150	
	20	750	150	
	30	1000	300	
			Q_{path} = 600	0.0057

TABLE VII

Comparison of observed and calculated Pn amplitude ratios from SHOAL using Q_{path} absorption in the upper mantle.

Station Designator	Initial Amplitude Reduction Factor	Observed Pn Amplitude	Amplitude Ratio Calculated	Observed
WINV	0.660	467.	1.000	1.000
BMSO	0.0039	30	.058	.063
HLID	0.0110	11	.017	.024
TKWA	0.0060	4.5	.009	.010
EKNV	0.437	1445	1.000	1.000
UBSO	0.0080	8.4	.018	.006
WINV	0.660	467	1.000	1.000
RYND	0.0020	47.5	.003	.101
HHND	0.0057	55.2	.087	.118
CUNV	0.218	1264	1.000	1.000
KNUT	0.0250	28	.115	.222
BXUT	0.0180	13	.082	.103
TFSO	0.0013	13	.006	.103
DRCO	0.0150	5.4	.069	.042
TDNM	0.0150	5.4	.069	.042
RTNM	0.0090	2.2	.041	.017
LCNM	0.0150	10.5	.069	.084
AZTX	0.0095	8.4	.044	.067
SKTX	0.0069	8.0	.032	.064
WMSO	0.0060	4.3	.028	.034
APOK	0.0024	(14.0)	.012	(.111)

Data to the southwest for the predicted ratios is the most
extensive, and it shows good agreement in pattern, if not ampli-
tude ratio, with the observed amplitude ratios. The gross
underestimate of the TFSO ratio has no ready explanation, except
that perhaps some unique interference conditions were present
in the measured signal, or that a very low amplitude earlier
arrival was not detected in the record analysis. Five stations
on the southeast profile show ratios which are low relative to
the predicted values (DRCO, TDNM, RTNM, AZTX, SKTX), indicating
that generalization of the contours in the loop of lower Q in
that region results in a Q which is slightly too high. It is
also possible that the strong radiation pattern noted may be a
contributing factor, since all of these stations are at a rela-
tively narrow azimuthal aperature with respect to the source and
the normalizing station is slightly outside of this aperature.
The predicted pattern of high and low amplitude closely corres-
ponds to that observed, however, and refinement of the contours
could, no doubt, improve the estimate significantly.

In any case, the amplitudes predicted agree among themselves,
and to a significant degree within the resolution of the contours.
The range of predicted values and the relative values of the
ratios are certainly no more scattered than those observed in the
original data, and perhaps even less scattered, suggesting that
the lateral variations of Q indicated here not only represent the
true upper mantle variations, but that the variations might be
used to improve estimates of event magnitude calculated from the
Pn wave.

8.   UPPER MANTLE Q FROM Pn BENEATH THE UNITED STATES

8.1 Discussion

Romney (1959, 1962) commented upon the apparent difference
in body wave attenuation in the eastern and western United States,
noting that Pn amplitudes from explosive sources were much less
attenuated in the east as compared to western regions. Molnar
and Oliver (1969) found that the amplitudes of the short-period
shear phase Sn, from earthquakes, which propagates along approx-
imately the same path as Pn, followed the pattern noted by Romney
with even greater emphasis of the attenuation differences. The
qualitative conditions established by these observations are
clearly reflected in the Q contours given in Figures 4 and 5,
with low values of upper mantle Q predominating in the western
region and high Q in the east. Certain areas within both the
eastern and western regions are found which contradict this
general statement which will be discussed later, but the overall
characteristics are unambiguous in principal.

In the western U.S., values of Q in the upper mantle given
by the method used here range from about 150 to 300 in the lower
velocity materials of the upper mantle, with calculated values
as low as Q = 10 and as high as Q = 410 excepting beneath part
of Utah. Values in the higher velocity materials range from
Q = 90 to Q = 670 in Arizona, from Q = 70 to Q = 860 in New
Mexico, and are estimated to be on the order of Q = 300 from
limited data beneath Nevada and southern Idaho. No reliable
values for either high or low velocity sections were observed in
California or other West Coast regions, but generally high Q for
north-south paths beneath California is indicated from a single
observation set from the Washington-Oregon border earthquake.

Upper mantle Q east of the Rocky Mountains ranges in calcu-
lated values from 500 to 1000 or greater for the most part, with
Q greater than 1000 suggested for much of the eastern region.
Exceptions to high Q in the east are apparent in the Texas-

Louisiana border region and in a tentative band of low Q
extending from northern Minnesota through central Missouri.

8.2 Earlier Determinations of Upper Mantle Q

A few determinations of upper mantle Q beneath the United
States have been published, and among those are Dorman (1968),and
O'Brien (1968) in the eastern U.S. Dorman estimated upper
mantle Q (above 126 kilometers) at Q = 475 with 90% confidence
limites of 300 and 1100 for the Lake Superior region. O'Brien
found that an assumed Q of 1000 generally agreed with amplitude
attenuation southwestward from Lake Superior toward Arizona.
These values agree with the contours of upper mantle Q given in
Figure 4 for the high velocity Pn.

Kanamori (1967a, b), Archambeau, et al. (1969), Anderson,
et al. (1965), Long and Berg (1969), and Johnson and Couch (1970)
have published upper mantle Q estimates for the western U.S.
Results obtained from surface wave attenuation by Anderson, et al.
in Arizona agree with Kanamori's estimates from core-reflected
body waves of Q = 100, and generally with Long and Berg's estimate
of Q for the same region of about 169 in the upper mantle. East
of the Nevada Test Site, Long and Berg found upper mantle Q on
the order of 116. Archambeau, et al., found that Q in paths
leading out of the Nevada Test Site generally ranged from 300 to
500 in paths not covered by the other results cited. Upper
mantle Q contours given in Figures 4 and 5 show essentially the
same values for each particular determination, even though the
more sophisticated spectral techniques were used for the results
given as comparisons. The rather limited data obtained in this
work result in an upper mantle Q estimate for the Pacific North-
west which also agrees with a more detailed determination of
upper mantle Q from Pn obtained by Johnson and Couch in the
northern Cascades of Q = 383 $\pm$ 41.

8.3 General Relationships with Other Factors

Patterns of the contours of upper mantle Q showing the lateral variation of this factor describe provinces in the upper mantle much in the same way that physiographic characteristics can be selected to define distinct regions. In fact, there is a correspondence of Fennemans (1931, 1938) physiographic province boundaries with observation of changes in crustal structure, crust and upper mantle seismic velocities, the gravity field, and many other geophysical and geological observations which leads immediately to the conclusion that all are interrelated to the extent that conditions in any one are likely to be reflected in some way in the others. This is hardly a unique conclusion (see Hales, et al., 1968, for an example), but some relationships are mentioned below to show a few aspects of the principle.

Crustal instability indicated by historical seismicity and the obvious structural activity during Cenozoic time in the Basin and Range are clear indications of some kind of mobility in the upper mantle beneath this region. The structural relief could hardly be accomodated in the crust of the region alone. Total magnetic field intensities over the Basin and Range suggest that the Curie geotherm is shallow here relative to the eastern U.S. (Zietz, 1969; Pakiser and Zietz, 1965), a suggestion which is supported by the interpretation of high heat flow from within the earth by Roy, et al. (1968) for this region. Any particular mineral assemblage constituting the upper mantle rock is unlikely to have the same density under a high temperature environment as it would in low temperatures, particularly if it were confined in volume only by it's elastic properties and a fractured and mobile crustal overburden. The density difference is reflected by a broad negative Bouguer gravity anamoly (see Woollard, 1966) and, accordingly, the velocity of Pn beneath the Basin and Range is anamously low (Herrin and Taggart, 1962). Each observation leads to the conclusion that the upper mantle beneath this region is

not a stable, rigid platform supporting the crust.

The pattern of amplitude absorption of the Pn wave found in this study, particularly in the low velocity Q contours (Figure 5), clearly corresponds to the surficial and crustal character- istics typifying the Basin and Range. Virtually all Q values less than about 150 are found here. The limits of Basin and Range structure are given by rapid lateral increases of Q beneath the Columbia Plateau-Snake River Plains provinces to the north and beneath the Colorado Plateau east and north of the central and southern Basin and Range. Observations of very low Q in the upper mantle in northwestern New Mexico correspond to a north trending reentrant of Basin-Range structure in that area as a subtle indication of the strength of the interrelationship.

In contrast to the rugged, high relief noted in the west, the physiography of the United States east of the Rocky Mountain front reflects crustal (and hence subcrustal) stability for the most part during Cenozoic time. The lack of strong local relief in the east reflects either an abscence in the past of such relief or that a sufficient amount of time has passed for the relief to be muted by long term erosional processes. Sedimentary unit thicknesses and lithological characteristics also vary little with lateral distance for the most part, again contrasting with the western region characteristics. Intrusive and extrusive activity in the east during Cenozoic time are also at a minimum in comparison. The geological aspects clearly point to relative stability, as do the geophysical observations.

9. COMPARISON OF UPPER MANTLE Q WITH OTHER GEOPHYSICAL OBSER-
    VATIONS.

9.1 Comments

Attenuation differences in the upper mantle shown by the
contours of Q may be expected to influence all seismic energy
propagating through upper mantle regions. The attenuation obvi-
ously can affect amplitudes, but it may also be reflected in
traveltimes of energy passing through the materials of different
elastic qualities indicated by the Q measure. A comparison of Q
with amplitude and traveltime data might therefore show some
relationship compatible with what is known or suspected from the
distribution of Q.

9.2 Teleseismic P-Wave Amplitudes

A strong correlation exists between the relative attenuation
of teleseismic P-wave amplitude and the Q values determined from
the Pn phase. One recent amplitude attenuation study (Evernden
and Clark, 1970) utilized the P-wave signals from over 70 earth-
quakes recorded by many stations common to the data used here
for Q determination. Many other amplitude studies have also been
made (see Herrin, 1969, and others), and the general trends are
compatible with each other. Evernden and Clark presented their
relative amplitudes as the logarithm of the amplitude difference
observed at some station compared to amplitude at a reference
station, corrected for the distance difference. Data is taken
from their Figure 1 and re-plotted in Figure 6 for comparison
with the Q contours. Very good agreement in some detail is
observed: Negative logarithms (low relative amplitudes) corres-
pond almost without exception to the low Q regions. One possible
exception is present in southernmost Utah where Q in the low
velocity material is apparently changing very rapidly. Positive
logarithms, representing high relative amplitudes, clearly
correspond to high Q regions. The trough of low Q extending from
southern Colorado through eastern Oklahoma is paralleled by
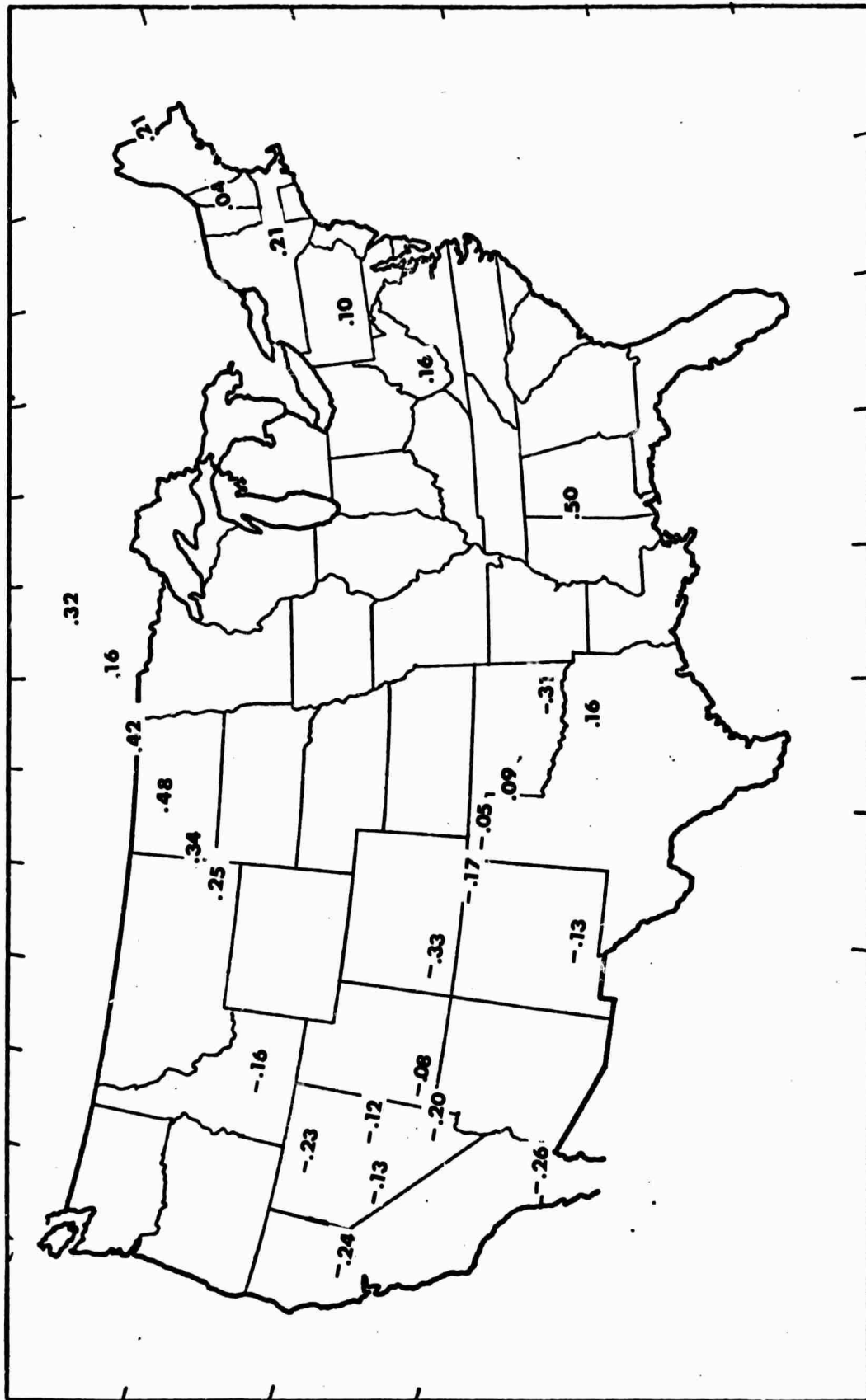
Figure 6. Logarithms of the relative amplitudes of teleseismic
P-waves observed by Evernden and Clark

negative logarithmic values, and an indication of low Q north-
west of the Great Lakes is reflected by somewhat lower amplitudes
in comparison to the North Dakota and Montana values.

9.3 Traveltimes of Teleseismic P-Waves

Traveltimes of teleseismic P-waves also agree in detail with
the Q values obtained from Pn. The procedure for investigation
traveltimes is quite simple: A traveltime curve is chosen or
developed, and differences observed from the traveltime indicated
by the curve are accumulated as a measure of relative delays in
different regions. Such data are reproduced from Herrin and from
Archambeau, et al., contours of Cleary and Hale's (1966) data in
Figure 7. The patterns are somewhat different, both as a result
of the traveltime curve selected and observing station distribu-
tion. The major feature always observed in such studies is that
traveltimes to observation points in the east are early in compar-
ison to traveltimes observed in the west. These general features
correspond to the high and low Q regions, respectively.

P-wave delay pattern agreement with the Q contours is very
good, even in some detail where Q values are least well determined.
To point out a few of the more subtle areas of agreement,
Archambeau, et al.'s relatively early teleseismic P arrivals in the
northwestern United States corresponds to moderately high Q from
limited data, and the eastward swing of low Q into the West
Virginia-Pennsylvania mountain region corresponds to contours of
delay indicating a decrease in the amount of "earliness" of the
P-wave. This effect is even more pronounced in Herrin's contours,
with very good agreement evident. No strong correlation in the
Texas-Oklahoma region is found in any of the P delay maps or
tabulations in published literature.

It is especially interesting to note that the low Q contours
in Nevada and Arizona (Q = 150) are very good replicas of the
+ 0.6 second relative P-wave delay given by Archambeau, et al.,
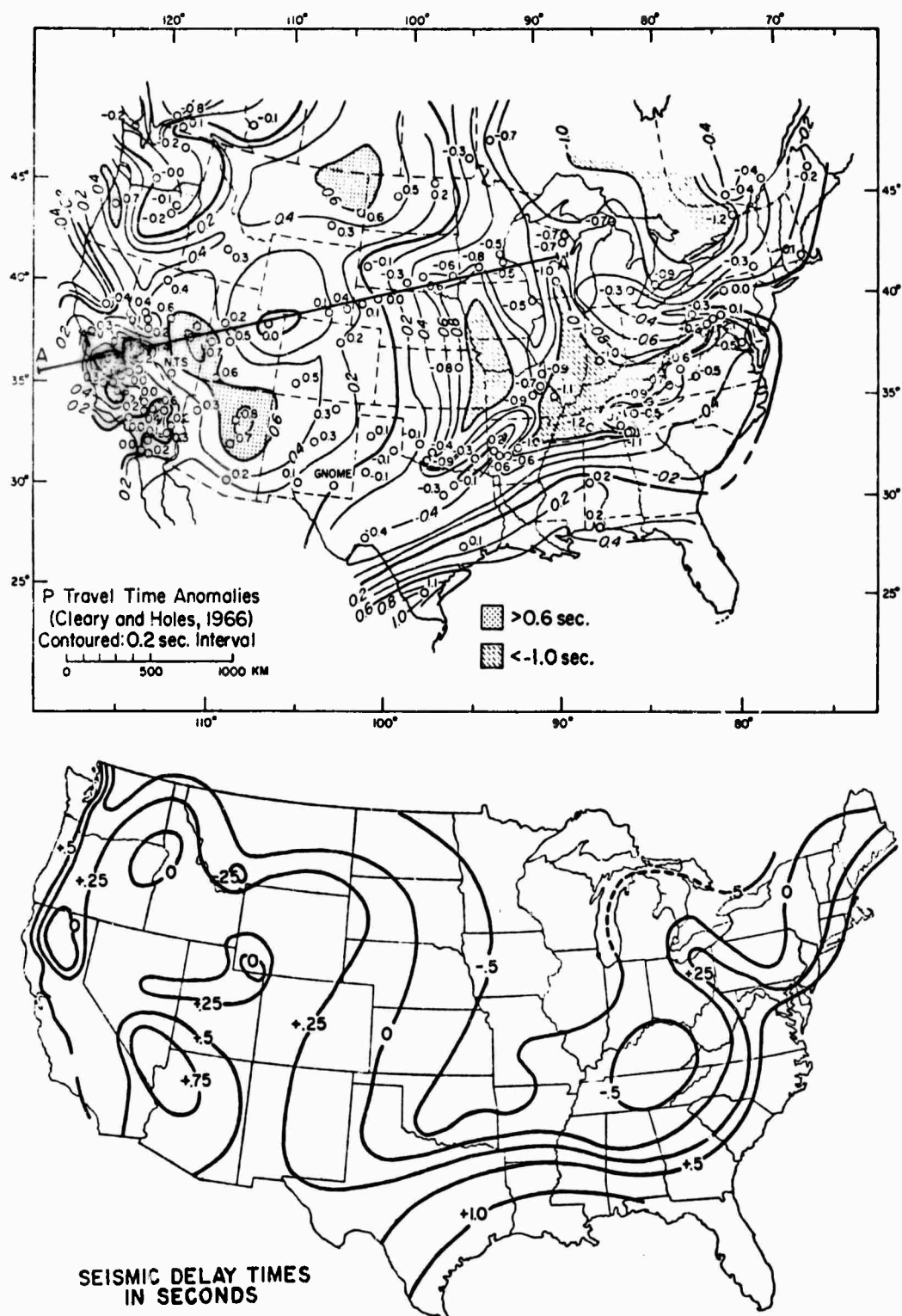indicating the strong influence of the lower velocity materials

Figure 7. Relative delay times of teleseismic P for the United States after Archambeau, _et al._, (top) and Herrin (bottom).

upon both Q and traveltimes. The very high values of Q in the Colorado Plateau (Utah) are not very strongly indicated by delay times, but a zero reference in delay times is close to this region and details may be obscured for that reason. The geographical region where maximum relief of Q in the low velocity materials and "maximum lateness" of arrival times for P do correspond both here and in Herrin's results, however, and a close relationship is clearly indicated.

9.3.1 A Brief Aside: Perhaps most suprisingly in view of the limited Q data showing low values in the central U.S., the band of implied low Q shown in Figure 5 has a clear influence upon P-wave delays given by Archambeau, et al. A band of less early P arrivals surrounded by very early P arrivals outlines the low Q band quite well. Details at the southern extent of the band, in the Arkansas region, do not appear to be in agreement with the Q data. The band itself is not reflected in Herrin's contours, possibly because of different station distributions.

This band of low Q requires a different interpretation than that given for Q of nearly the same values in the west. No other observations of gravity, heat flow, magnetics, or velocities seems to correspond to the very low values in this region, suggesting some factor other than upper mantle rigidity is dominating the amplitude trends observed. Since correlation with teleseismic P times is noted, an alternate cause for strong Pn amplitude loss in paths traversing the region may exist.

Lowest values of Q in the band are found in the Illinois-Missouri region where historical records show a relatively high incidence of seismic activity relative to most of the rest of the central United States (see Nuttli, 1965; Kisslinger and Nuttli, 1965). Lacking any other observations which would lead to an interpretation of mantle instability related to subcrustal heat and related factors, the fact may be that the assumption of lateral upper mantle homogeniety is not sufficiently justified for

paths in this region. Structural elements related to the observed seismic activity which extend to depths where Pn propagates may be the cause of the amplitude loss through scattering and mode conversions of the Pn wave at the extended fault boundaries.

If such an interpretation is valid, the effect upon teleseismic P-wave traveltimes would lead to the suggestion that ruptures in the crust evidenced by the seismic activity might well extend to considerable depths in the mantle. There are no data presented here to support such a conclusion beyond the correlation of low Q and P-delays. The extension of the possibility of upper mantlw faulting in a norhterly direction can also be only implied by the contours in Figure 5, since even the related seismicity is lacking. The northerly trend is supported, however, in observations of the Q determined from upper mantle paths of the Pn wave.

9.4   Traveltimes of Teleseismic S-Waves

Studies of teleseismic S-wave delays which are derived in much the same way as those for P also show features of interest to the upper mantle Q results. Delay times of teleseismic S might be expected to show more correlation with the Q than P delays since the shear velocity is a much stronger function of the rigidity. If the contours in Figures 4 and 5 are compared to the teleseismic S-wave delays given by Hales and Roberts (1970), gross details of the patterns correspond. Contours of S-wave delay for comparison are given in Figure 8.

Earliest S-wave arrivals correspond to regions of high Q, and the very latest arrivals correspond to the lower Q found in Arizona. Details of the figure do not agree as well as in the P-wave comparison, and the reason may lie in the measurement of long-period S-wave arrival times which are difficult to time because of the emersive nature of the wave onset. The higher Q in Washington corresponds to relatively early S times, but neither the Nevada or Texas-Oklahoma low Q trends compare to the S contours favorably. The band of low Q in the central United States is not even suggested by the S-delay contours, and the West Virginia-Pennsylvania P-wave and Q trends are directly contradicted by the S-wave delays. Solomon and Tolsoz also present evidence that the central band of low Q surrounds a location where the earlies S-wave arrivals are found in the relative teleseismic times from two South American Earthquakes.

Strong association of Q with P delays and even stronger association with S-wave delay is expected from theoretical considerations of wave velocities (Knopoff; Anderson; Jackson and Anderson) but the relationship can be demonstrated only in the western region from the data here. The mechanism for amplitude loss may be partial melting along grain boundaries or other loss of between-grain cohesion, in effect reducing the bulk shear strength and lowering the effective rigidity. Such a loss in
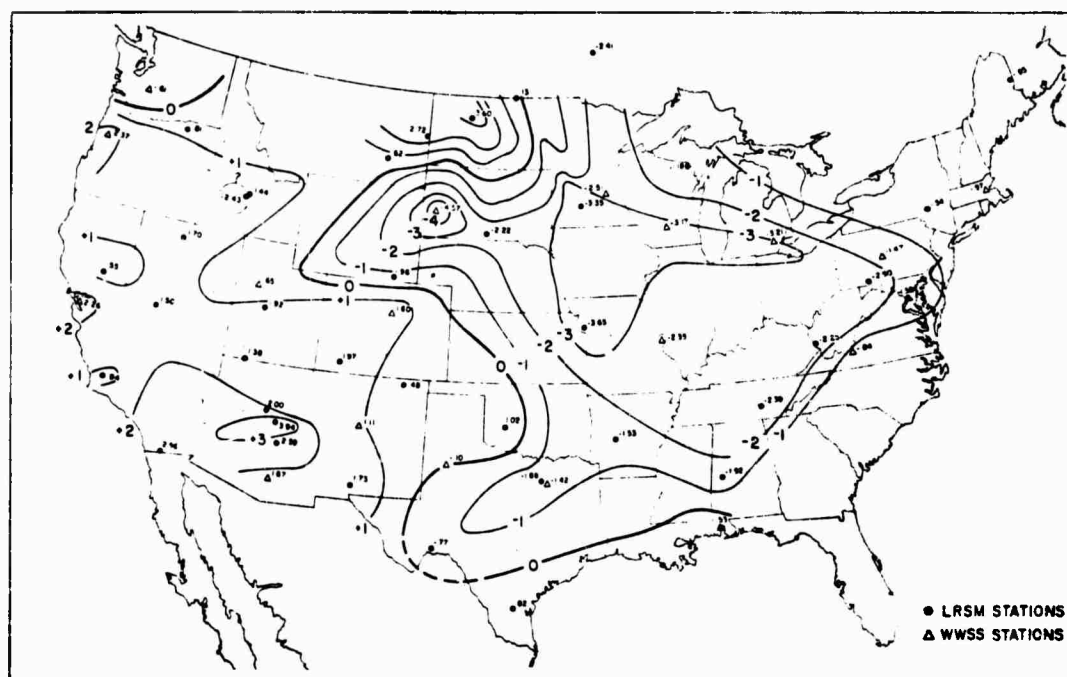
Figure 8. Relative delay times of teleseismic S for the
United States, after Cleary and Hales.

rigidity has a very strong effect upon shear wave velocity
compared to compressional velocity.

High subcrustal temperatures are implied by partial melting,
and such an hypothesis for regions in the upper mantle beneath
the western United States have been advanced before (see Knopoff,
Julian, 1970; Julian and Anderson, 1968; hales and Doyle, 1967).
The possibility certainly exists according to the indication of
two different values of Q for certain of the western regions, and
further comparison with other observations in that region gives
some support to the view in additional detail below.

9.5 Comparison of Upper Mantle Q and Regional Heat Flow

Heat flow from within the earth is typiclly low in the east-
ern United States according to Horai and Simmons (1969), with
values generally ranging from 0.4 - 1.8 HFU (HFU = Heat Flow Unit
= microcalorie/centimeter^2/second). Measurements are not avail-
able in the detail needed to compare directly with the Q contour
pattern, but high Q does correspond to low heat flow as would be
expected in a relatively cool, stable mantle. On the other hand,
the western United States is typified by high and variable heat
flow which is likely related to continuing development of the
crustal structures.

Heat flow in the western U.S. has been summarized by Roy,
et al., (1970) and Blackwell (1971). Their data are summarized
in Figure 9 as regions of high heat flow (greater than 2 HFU) and
low heat flow (less than 2 HFU) for comparison with the Q data.
Many details of the heat flow pattern coincide with the patterns
of Q, with trends to lowest Q values found in the high heat flow
regions in Idaho, Nevada, Arizona, and New Mexico. The Utah
region of high Q corresponds, at least in part, to low heat flow
values, but extension of low heat flow into central Arizona
suggested by the contours is not indicated by Q results here.
The central Arizona region is quite variable in Q values as can
be seen in Table III, and is apparently also variable in heat flow

values as indicated by the necessity for dashed heat flow
contours in the figure. The northeastward trend of high heat
flow extending through southwestern Colorado corresponds to the
low Q values in the low velocity materials as shown in Figure 4,
but the Q data only imply the same trend in the higher velocity
plot.

9.6 Anomolous Magnetic Fields and Upper Mantle Q

Heat flow trends also show strong correlation with the mag-
netic field variations caused by induced currents within the
earth during geomagnetic stroms, as noted by Reitzel, et al.
(1970) and Porath (1970, 1971). Amplitude and wave length of the
induced currents and the anamolous magnetic fields resulting from
the currents reflect the resistivities of various regions within
the earth, providing a tool for examining some characteristics of
the earth as a conducting body. The resistivities of most
materials are a function of temperature to some extent, and the
observation that heat flow and anamolous magnetic fields caused
by the induced currents show correlation is not too suprising.
Since a close correspondance between upper mantle Q and heat flow
can be demonstrated, it also seems quite likely that there will
be some agreement between the anamolous field intensity and upper
mantle Q.

Figure 10 gives Reitzel's contours of the anamolous vertical
magnetic field intensity in gammas observed in the southwestern
United States during a geomagnetic substorm. The wave period is
60 seconds, which is estimated by Reitzel to be appropriate for
sampling the crust and uppermost mantle. An overlay of upper
mantle Q contours for the low velocity layer is also given in the
figure in heavy lines for comparison with the field intensity.
The agreement between trends is rather striking, with regions of
high upper mantle Q corresponding to high field intensity and
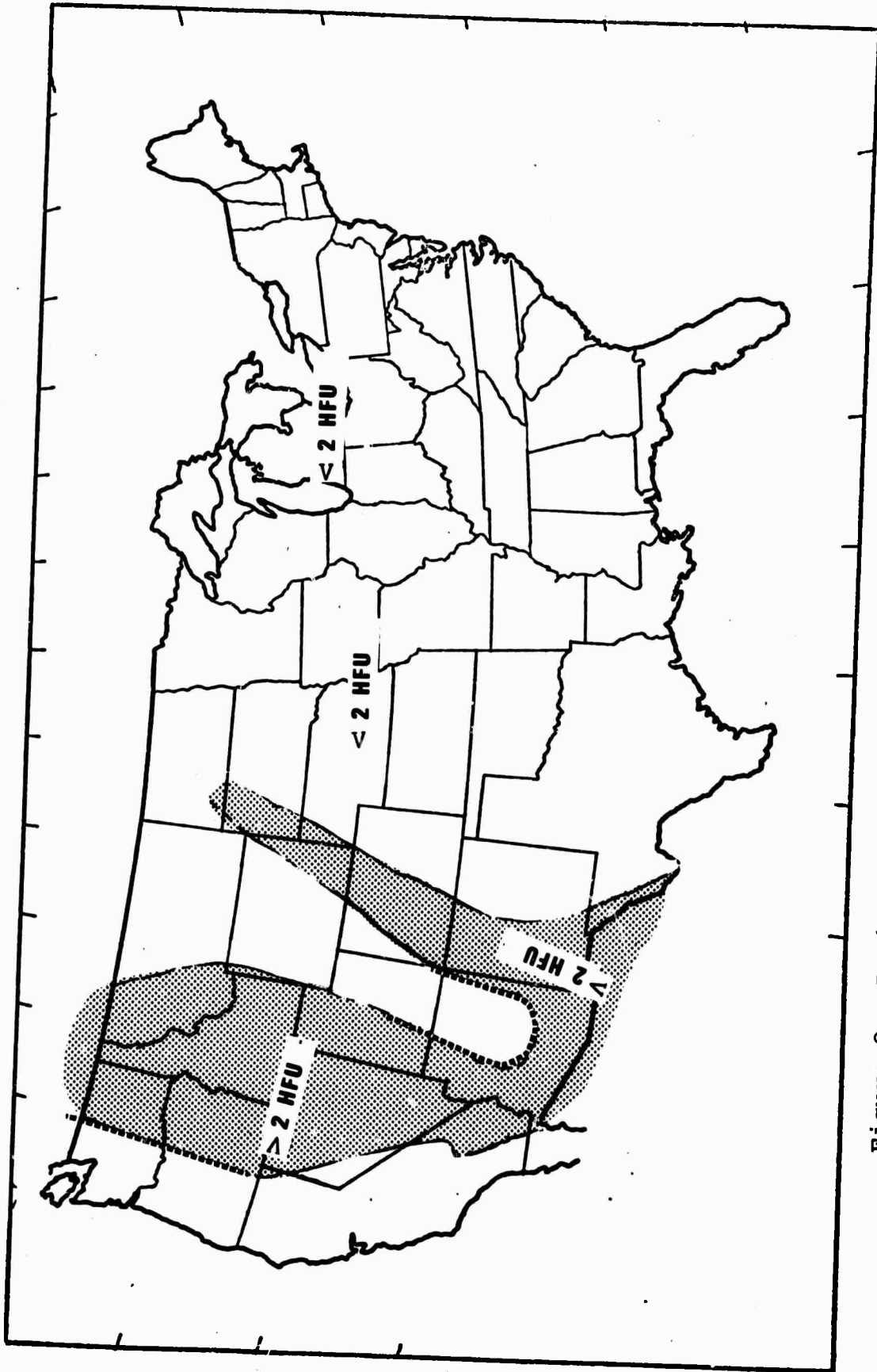regions of low Q corresponding to low field intensity trends.

Figure 9. Regional heat flow trends in the United States, after Blackwelder, et al.

Interpretation of the reasons for field intensity variations corresponds to that for Q, in that low Q may reflect high sub-crustal temperatures and partial melting, and low anamolous intensity occurs over regions where resistivity in the crust and upper mantle are low.

Porath (1971) calculated one crust-upper mantle resistivity structure which would result in the anamolous field intensities given by Reitzel. The profile A - A' in Figure 10 shows the location of Porath's model which is reproduced in the lower half of Figure 11. The model shows a layer of low resistivity materials which varies in thickness above a base at about 200 kilometers beneath the earth's surface sandwiched between a high resistivity crust and high resistivity mantle. Variations in the observed field intensity are assumed to be caused by variations in thickness of the low resistivity layer. Changes in resistance in a constant thickness layer could be modelled for the same result. The upper half of Figure 11 is a profile through the upper mantle Q contours along the same A - A' profile. The thin regions of Porath's model of the low resistivity layer correspond to regions of high upper mantle Q, and where a greater amount of low resistivity material is indicated by the field intensity, a low Q is also indicated. The comparison of upper mantle Q therefore corresponds to suggestions of partial melting from the field intensity trends, and the influence of subcrustal heating is reflected in both factors.
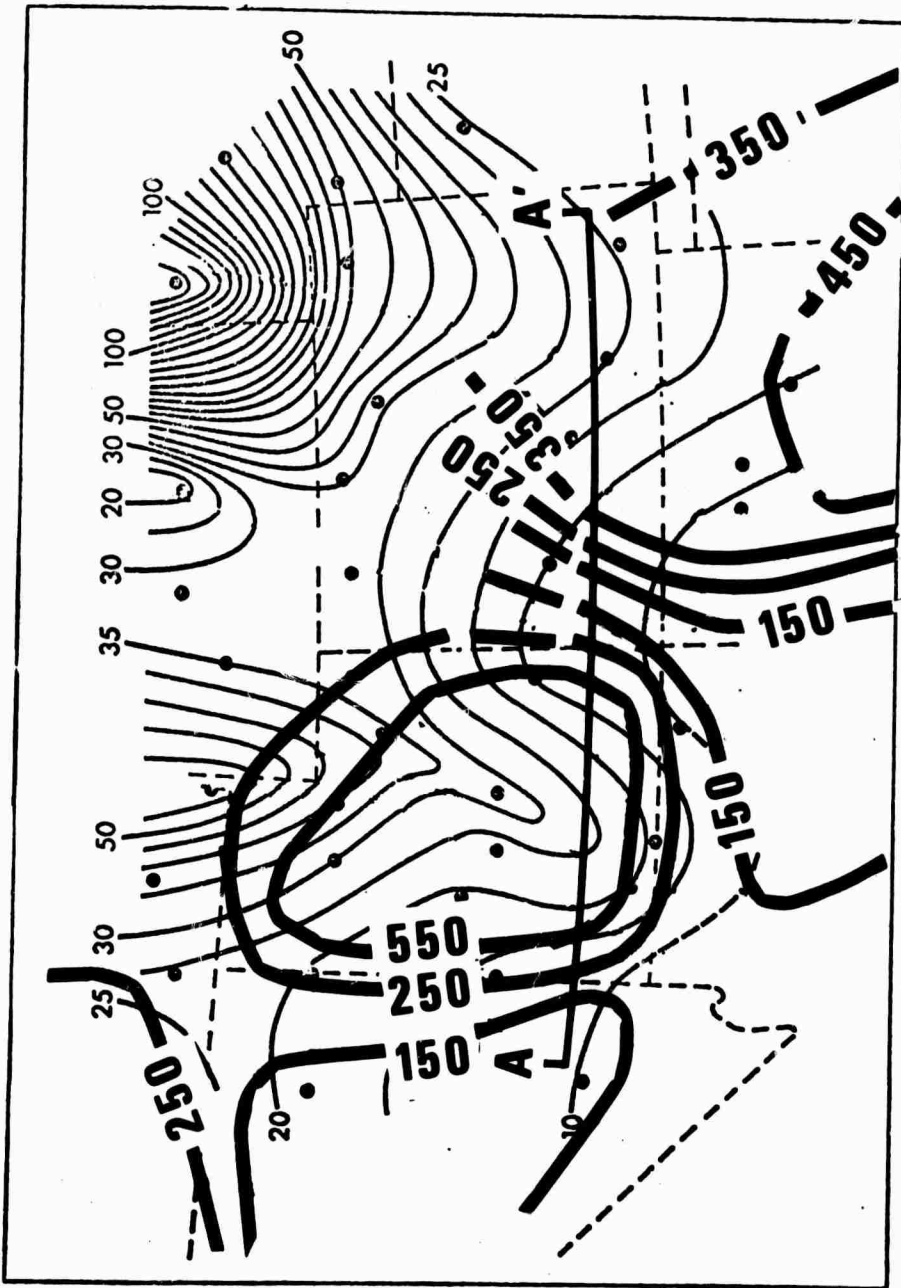
Figure 10. Anamolous vertical field intensity during a geomagnetic storm (in gammas) after Reitzel, et al., in light contours compared to contours of upper mantle Q from low velocity Pn.
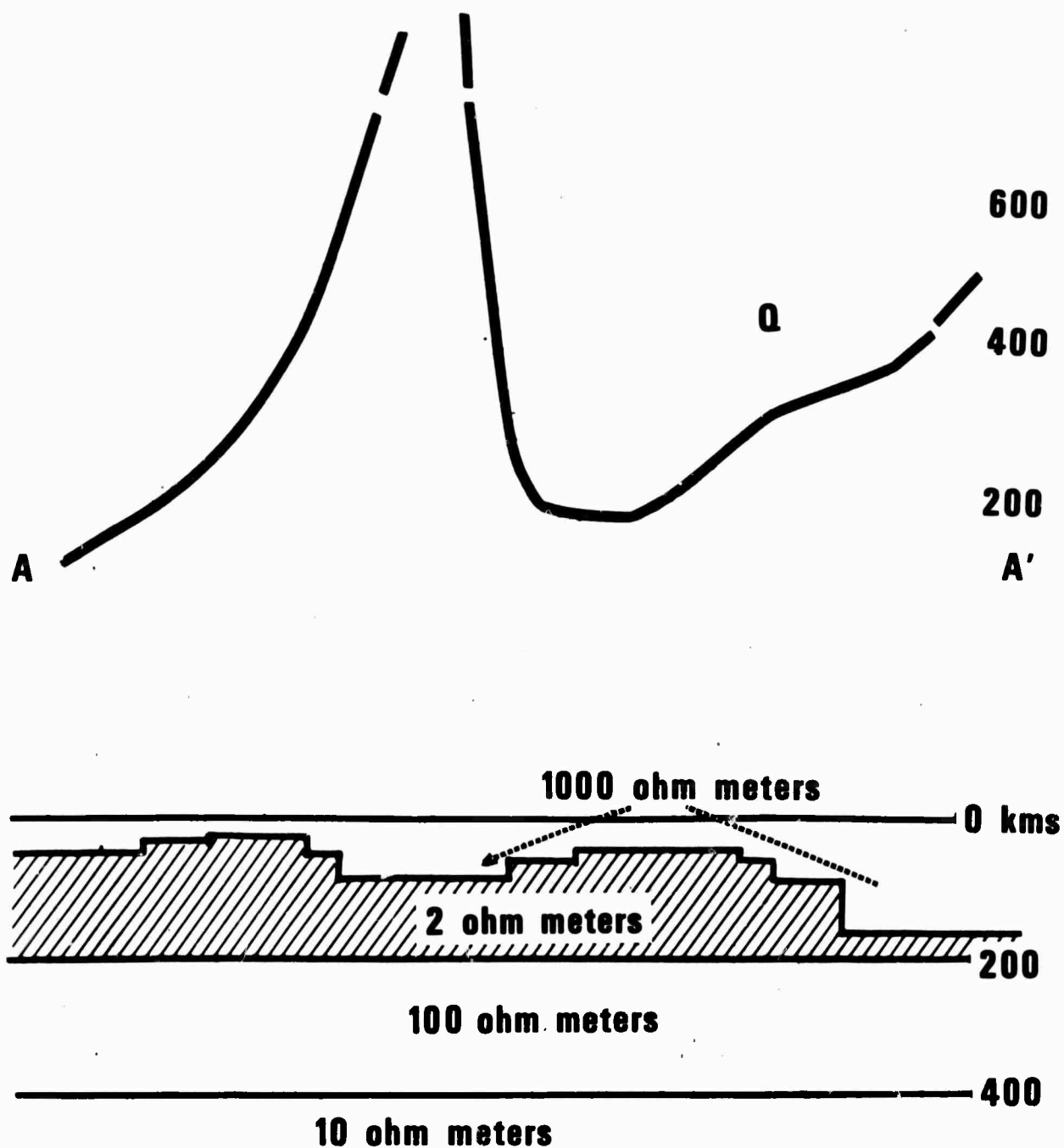
Figure 11. Profile A - A' through upper mantle Q contours in figure 10 compared to upper mantle resistivity model by Porath for the same profile.

10. <u>SUMMARY AND DISCUSSION</u>

Lateral variations in the seismic wave absorption factor Q
are clearly expressed by amplitude variations of the Pn phase as
it propagates in the upper mantle beneath the United States.
When the phase is assumed to be a head wave with amplitude
decreasing approximately as the inverse square of distance, the
amplitude drop in excess of this spreading factor closely reflects
upper mantle conditions implied by the observations of other
seismic and non-seismic factors. Such factors as the teleseismic
wave amplitudes and relative delay times appear to be related to
heat flow rates from the interior of the earth. Details of heat
flow patterns are also reflected by details in the pattern of
geomagnetically induced earth currents in a frequency range
dictating that major influences upon the resulting magnetic fields
are in the upper mantle of the earth. Close correspondence with
each of these factors can be demonstrated in upper mantle Q
determined from the Pn phase. Use of the Pn wave as a tool for
mapping the lateral variations of upper mantle Q is therefore
justified, and the possibilities for further understanding of
physical conditions beneath the crust are significantly improved.

Perhaps one of the most significant results noted in the data
is the agreement between upper mantle Q and the teleseismic
signal amplitudes and relative delays. According to theory, Pn
propagates wholly within the upper mantle, following a path
closely paralleling the crust-mantle interface. Since only those
materials a few kilometers beneath this boundary can influence the
Pn wave amplitude, the agreement with teleseismic data indicates
that Q from Pn may be a good deal more representative of upper
mantle Q than suggested by it's path alone. Relative time delays
of the teleseismic P-wave on the order of seconds could hardly
occur within a zone only a few kilometers thick, and the general
characteristics of S-waves from teleseisms imply the same
conditions. Q from Pn may very well represent Q for a relatively

large part of the upper mantle, and if so, the ease of measuring
and calculating the necessary terms for the Q determination as
presented here makes a comprehensive mapping of the lateral
variations in upper mantle Q well within reach.

In attempting to project amplitudes on the basis of the con-
tours derived from the path data, some interesting possibilities
are presented. Sufficient detail in the contours could easily
provide a useful method of estimating seismic magnitudes at
regional and near-regional distances where the Pn pahse is the
first identifiable arrival on the seismogram. Such an approach
would remove the necessity of resorting to statistically derived
curves of amplitude decay with distance which must necessarily
accomodate a very wide scatter in amplitudes observed in most
seismic data. Additional paths and more knowledge of depths or
radiation pattern influence would be necessary to achieve such
a goal, but the method given here is simple, straightforward,
and easily applied.

More detail will also eventually evolve a much more perceptive
picture of the uppermost mantle and the contribution of this part
of the earth to the movements observed on and within the crust.
Certain limits in rheological properties are provided by the Q
measure. The possibility of new interpretations of crust-mantle
interaction is increased, since concurrence in the details of
models derived from different data bases increases confidence in
the results of each method.

11. REFERENCES CITED

Anderson, D. L., and C. B. Archambeau (1964), The anelasticity of the earth: J. Geophys. Res., 69, 2071-2084

_____,A. BenMenahem, and C. B. Archambeau (1965), Attenuation of seismic energy in the upper mantle: J. Geophys. Res., 70, 1441-1448

_____,(1967), The anelasticity of the mantle: Geophys. J., 14, 135-147

_____,(1971), Structure and composition of the mantle: Trans. Amer. Geophys. Un., 52, 174-175

Archambeau, C. B., E. A. Flinn, and D. G. Lambert (1969), Fine structure of the upper mantle: J. Geophys Res., 74, 5825-5866

Birch, F., and D. Bancroft (1938), Elasticity and internal friction of a long column of granite: Bull. Seism. Soc. Amer., 28, 243-254

Blackwell, D. D. (1971) Heat flow: Trans. Amer. Geophys. Un., 52, 135-139

Brekhoviskikh, L. M. (1953), Waves in Layered Media: transl. by P. L. Lebonion, Academic Press.

Bullen, D. E. (1947), An Introduction to the Theory of Seismology; Cambridge University Press.

Byerly, P. (1942), Seismology: Prentice-Hall, Inc.

Cleary, J. and A. L. Hales (1966), An analysis of traveltimes of P-waves to North American stations in the distance range 32 to 100 degrees: Bull. Seism. Soc. Amer., 56, 467-489

Evernden, J. F. (1967), Magnitude determination at regional and near-regional distances in the United States: Bull. Seism. Soc. Amer., 57, 591-639
_____ and D. Clark (1970), Study of Teleseismic P II. Amplitude data: Phys. Earth Planet, Interiors, 4, 24-31

Ewing, M., W. Jardetzky, and F. Press (1957), Elastic Waves in Layered Media: McGraw-Hill, Inc.

Fenneman, N. M. (1931), Physiography of Western United States; McGraw-Hill, New York.

_____ (1938), Physiography of Eastern United States; McGraw-Hill, New York

Grant, F. S., and G. F. West (1965) Interpretation Theory in Applied Geophysics: McGraw-Hill, Inc.

Gutenberg, B. (1924), Dispersion und Extinction von seismischen Oberflachenwellen und der Aufbau der oberster Erdschicten: Z. Phys., 25, 227-386

_____ (1945), Amplitudes of P, PP, and S and the magnitude of shallow earthquakes: Bull. Seism. Soc. Amer., 35, 57-69

_____ (1948), Attenuation of seismic waves in the earth's mantle: Bull. Seism. Soc. Amer., 48, 269-282

_____ (1951), The elastic constants of the interior of the earth, in Internal Constitution of the Earth: Dover Publishing

_____ (1958), Attenuation of seismic waves in the earth's mantle: Bull. Seism. Soc. Amer., 48, 269-282

Hales, A. H., and H. A. Doyle (1967) P and S traveltime anomalies and their interpretation: Geophys. J. R. A. S., 13, 403-415

_____ J. R. Cleary, H. A. Doyle, R. Green, and J. Roberts (1968), P-wave station anomalies and the structure of the upper mantle: J. Geophys. Res., 73, 3885-3896

_____ and J. L. Roberts (1970), Traveltimes of S and SKS: Bull. Seism. Soc. Amer., 60, 461-489

Heelan, P. A. (1953), On the theory of head waves: Geophys., 18, 871-893

Herrin, E., and J. Taggart (1962), Regional variations in Pn velocity and their effect on the location of epicenters; Bull. Seism. Soc. Amer., 52, 1037-1046

_____ (1969), Regional variations of P wave velocity in the upper mantle beneath the United States; in The Earth's Crust and Upper Mantle; Geophys. Mon. 13, 242-246

Hill, D. P. (1971), Velocity gradients and anelasticity from crustal body wave amplitudes: J. Geophys. Res., 76, 3309-3325

Horai, K., and Gene Simmons (1969), Spherical harmonic analysis of terrestrial heat flow: Earth Planet. Sci. Lett., 6, 386-394

Jackson, D. D., and D. L. Anderson (1970), Physical mechanisms of seismic wave attenuation: Ref. Geophys. Space Phys., 8, 1-63

Jeffries, H. T. (1929), The Earth: 2nd ed., Cambridge University Press.

_____ (1931), Damping in bodily seismic waves: Geophys. Suppl. J. R. A. S., 2, 318-323

Johnson, S. H. , and R. W. Couch (1970), Crustal Structure in the northern Cascade Mountains of Washington and British Columbia from seismic refraction measurements; Bull. Seism. Soc. Amer., 60, 1259-1269

Julian, B. R., and D. L. Anderson (1968), Traveltimes, apparent velocities, and amplitudes of body waves: Bull. Seism. Soc. Amer., 58, 339-366

_____ (1970), Regional variations in upper mantle structure in North America: Trans. Amer. Geophys. Un. (abs), 51, 359

Kanamori, H., (1967a), Spectrum of P and PcP in relation to the mantle-core boundary and attenuation in the mantle: J. Geophys. Res., 72, 559-571

_____ (1967b), Spectrum of short-period core phases in relation to attenuation in tne mantle: J. Geophys. Res., 72, 559-571

Kisslinger, C., and O. W. Nuttli (1965), The earthquake of October 21, 1965, and Precambrian structure in Missouri: Earthquake notes, 36, 32-36

Knopoff, L. (1956), The seismic pulse in materials possessing solid friction: Bull. Seism. Soc. Amer., 46, 175-183

_____ (1964), Q: Quart. Rev. Geophys., 2, 625-660

Kolsky, H. (1953), Stress Waves in Solids: Clarendon Press, Oxford.

Long, L. T., and J. W. Berg (1969), Transmission of the primary seismic wave 100 to 600 kilometers; Bull. Seism. Soc. Amer., 59, 131-146

Molnar, P., and J. Oliver (1969), Lateral variation of attenuation in the upper mantle and discontinuities in the lithosphere; J. Geophys. Res., 74, 2648-2682

Nagoka, H., (1906), On damped pregressive waves and the formation of tail in distant earthquakes: Proc. Tokyo Mat.-Phys. Soc., 13, 17-25

Nutti, O. W. (1965a) The southern Illinois earthquakes of August 14 and 15 1965 (Abstract): Earthquake Notes, 36:26

O'Brien, P. N. S. (1968), Lake Superior crustal structure-A reinterpretation of the 1963 experiment: J. Geophys. Res., 73, 2669-2960

Pakiser, L. C., and I. Zietz (1965), Transcontinental crustal and upper mantle structure: Rev. Geophys., 3, 505-520

Pasechnik, I. P., (1970), Characteristics of seismic waves from nuclear explosions and earthquakes: in Geosciences Bulletin, Series A, 1: Rand Corporation

Porath, H., D. W. Oldenburg, and D. I. Gough (1970), Separation of magnetic variation fields and conductive structures in the western United States: J. Geophys. Res., 76, 2643-2648

_____ (1971), Magnetic variation anomolies and seismic low velocity zone in the western United States: Geophys. J., 19, 237-260

Press, F. (1964), Seismic wave attenuation in the crust: J. Geophys. Res., 69, 4417-4418

Reitzel, J. S., D. I. Gough, H. Porath, and C. W. Anderson (1970), Geomagnetic deep sounding and upper mantle structure in the western United States: Geophys. J., 19, 213-236

Ricker, N. (1949), Attenuations and amplitude of seismic waves: Trans. Amer. Geophys. Un., 30, 184-186

Romney, C. F. (1959), Amplitudes of seismic body waves from underground nuclear explosions: J. Geophys. Resl, 64 1489-1498

_____, B. G. Brooks, R. H. Mansfield, D. S. Carder, J. N. Jordan, and D. W. Gordon (1962), Traveltimes and amplitudes of principal body phases recorded from GNOME: Bull. Seism. Soc. Amer., 52, 1057-1074

Roy, R. F., E. R. Decker, D. D. Blackwell, and F. Birch (1968), Heat Flow in the United States: J. Geophys. Resl, 73, 5207-5221

Solomon, S. C., and M. N. Toksoz (1970), Lateral variation of attenuation of P and S waves beneath the United States: Bull. Seism. Soc. Amer., 60, 819-838

Sutton, G. H., W. Mitronovas, and P. W. Pomeroy (1967), Short-period seismic energy radiation patterns from underground nuclear explosions and small magnitude earthquakes: Bull. Seism. Soc. Amero, 57, 249-267

Teng, T. (1969), Attenuation of body waves and Q structure of the mantle: J. Geophys. Res., 73, 2195-2208

Woolard, G. P. (1966), Regional isostatic relations in the United States, in The Earth Beneath the Continents, Geophys. Mon. 10, Amer. Geophys. Un., 557-594

Zietz, I. (1969), Aeromagnetic investigations in the earth's crust, in The Earth's Crust and Upper Mantle, Geophys. Mon 13, Amer. Geophys. Un., 414-415